

Review

Carboxylic Ester Hydrolases in Bacteria: Active Site, Structure, Function and Application

Changsuk Oh ¹ , **T. Doohun Kim** ^{2,*} and **Kyeong Kyu Kim** ^{1,*} ¹ Department of Molecular Cell Biology, Sungkyunkwan University School of Medicine, Suwon 16419, Korea; changs.oh@gmail.com² Department of Chemistry, College of Natural Science, Sookmyung Women's University, Seoul 04310, Korea

* Correspondence: doohunkim@sookmyung.ac.kr (T.D.K.); kyeongkyu@skku.edu (K.K.K.)

Received: 4 October 2019; Accepted: 7 November 2019; Published: 14 November 2019



Abstract: Carboxylic ester hydrolases (CEHs), which catalyze the hydrolysis of carboxylic esters to produce alcohol and acid, are identified in three domains of life. In the Protein Data Bank (PDB), 136 crystal structures of bacterial CEHs (424 PDB codes) from 52 genera and metagenome have been reported. In this review, we categorize these structures based on catalytic machinery, structure and substrate specificity to provide a comprehensive understanding of the bacterial CEHs. CEHs use Ser, Asp or water as a nucleophile to drive diverse catalytic machinery. The $\alpha/\beta/\alpha$ sandwich architecture is most frequently found in CEHs, but 3-solenoid, β -barrel, up-down bundle, $\alpha/\beta/\beta/\alpha$ 4-layer sandwich, 6 or 7 propeller and α/β barrel architectures are also found in these CEHs. Most are substrate-specific to various esters with types of head group and lengths of the acyl chain, but some CEHs exhibit peptidase or lactamase activities. CEHs are widely used in industrial applications, and are the objects of research in structure- or mutation-based protein engineering. Structural studies of CEHs are still necessary for understanding their biological roles, identifying their structure-based functions and structure-based engineering and their potential industrial applications.

Keywords: carboxylic ester hydrolase (CEH); carboxylic ester; Protein Data Bank (PDB); crystal structure; active site

1. Introduction

Carboxylic ester hydrolases (CEHs, EC 3.1.1.-) are catalysts that hydrolyze linear and cyclic carboxylic ester bonds to produce carboxyl groups ($-\text{COOH}$) and alcohol groups ($-\text{OH}$) at termini. CEHs are found in all living organisms, including vertebrates, insects, fungi, plants, archaea and bacteria. Hydrolysis by CEHs is important for metabolite regulation [1], signal transduction [2], protein synthesis [3], stem elongation [4] and thermal stress response [5]. Offensive and defensive interactions between insects and plants are also mediated by CEHs [6]. Bacteria use CEHs to demolish cell walls and membrane structures for food uptake [7], and to infect hosts [8–10]. The functional diversity of CEHs is mediated by substrate specificities on various biomolecules, such as carbohydrates [11], lipids [12], polypeptides [13,14], nucleic acids [15] and other small molecules [16]. Their catalytic reaction is followed by the cooperation of catalytic residues including a classical Ser-His-Asp triad and substrate-binding residues.

In this review, we classified 136 bacterial CEHs deposited in the Protein Data Bank (PDB) [17] based on the source, their Enzyme Commission (EC) number, substrate, localization, active site structure, physiological function and three-dimensional (3D) structure, in order to provide a general overview of bacterial CEHs. In addition, their potency for industrial application is discussed.

2. Sampling of Bacterial CEH Structures in the Protein Data Bank

The structures of 525 bacterial enzymes belonging to the EC 3.1.1.- group were released in the PDB database until 2019 July. The 518 structures were identified using X-ray crystallography (XRC), and seven structures were identified using nuclear magnetic resonance (NMR). Here we only focused upon crystal structures. According to the PDB description (www.RCSB.org), EC numbers are assigned based on UniProtKB, GenBank, the Kyoto Encyclopedia of Genes and Genomes (KEGG), and authors' descriptions. Among 518 structures, 91 of them, such as metallo- β -lactamase, have been excluded, because they were reported to have other enzymatic roles that did not describe CEH activity. Theoretical structures (e.g., 1A20) are not analyzed. CEHs not annotated with an EC number, such as carbohydrate esterase SmAcE1, are also beyond the scope of this review, although they do have esterase activity [18]. As a result, 424 structures of 136 CEHs from 52 genera and metagenomic (uncultured and unidentified) samples were selected for the analysis, and 136 CEHs were classified based on EC numbers (Table 1). When several crystal structures were available in one enzyme (several PDB codes), the first reported structure was used as a CEH structure. Their sequences containing tag or mutation were analyzed after being recovered to wild type sequences. Exceptionally, the sequences were not recovered when the mutations in the active sites of CEHs induced a gain of function. The majority of the crystal structures were identified in 1.0–3.0 Å resolution, and even extremely high resolution (below 1 Å) cases were also reported (Figure 1A). The major bacterial sources of CEHs in this analysis are *Pseudomonas* (9.6%), *Bacillus* (8.8%) and *Geobacillus* (7.4%), as shown in Figure 1B. Ten CEHs (7.4%) originate in metagenomic samples.

Table 1. List of 424 Protein Data Bank (PDB) codes in carboxylic ester hydrolases (CEHs).

EC Number	Enzyme Function	PDB Codes
EC 3.1.1.-	carboxylic ester hydrolases	1C7I[19], 1C7J[19], 1ESC[20], 1ESD[20], 1ESE[20], 1QE3[19], 2A7M[21], 2WAA[22], 2WYL[23], 2WYM[23], 3DHA[24], 3DHB[24], 3DHC[24], 3DNM[25], 3F67, 3FAK[26], 3G9T, 3G9U, 3G9Z, 3GA7, 3H17[27], 3H18[27], 3H19, 3H1A, 3H1B, 3H2G[28], 3H2H[28], 3H2I[28], 3H2J[28], 3H2K[28], 3I2F[29], 3I2G[29], 3I2H[29], 3I2I[29], 3I2J[29], 3I2K[29], 3IDA[30], 3K6K, 3L1H, 3L1I, 3L1J, 3LS2 ¹ [31], 3PF8[32], 3PF9[32], 3PFB[32], 3PFC[32], 3PUH[33], 3PUI[33], 3QM1[32], 3S2Z[32], 4F21[34], 4KRX[35], 4KRY[35], 4OB6[36], 4OB7[36], 4OB8[36], 5A2G[37], 5HC0[38], 5HC2[38], 5HC3[38], 5HC4[38], 5HC5[38], 5MAL ² [39], 5UGQ[40], 5UNO[40], 5UOH[40], 6EHN[41], 6GRY[42]
EC 3.1.1.1	carboxylesterase	1AUO[43], 1AUR[43], 1EVQ[44], 1L7Q[45], 1L7R[45], 1R1D, 1TQH[46], 2H1I, 2HM7[47], 2R11, 3CN7[48], 3CN9[48], 3DOH[49], 3DOI[49], 3KVN[50], 4BZW[51], 4BZZ[51], 4C01[51], 4C87[52], 4C88[52], 4C89[52], 4CCW[53], 4CCY[53], 4FHZ[54], 4FTW[54], 4IVI[55], 4IVK[55], 4JGG[56], 4OU4[36], 4OU5[36], 4ROT, 4UHC[57], 4UHD[57], 4UHE[57], 4UHF[57], 4UHH[57], 4V2I[58], 4YPV[59], 5AO9[60], 5AOA[60], 5AOB[60], 5AOC[60], 5DWD, 5EGN, 5GMX[61], 5H3B[62], 6AAE[63], 6IEY[63]
EC 3.1.1.2	arylesterase	1VA4 ³ [64], 2Q0Q[65], 2Q0S[65], 3HEA ³ [64,66], 3H14 ³ [66], 3IA2 ³ [67], 3T4U ³ , 3T52 ³ , 4ROT, 4TX1[68]
EC 3.1.1.3	triacylglycerol lipase	1CVL[69], 1EX9[70], 1HQD[71], 1I6W[72], 1ISP ⁴ [73], 1JI3[74], 1KU0[75], 1OIL[76], 1QGE, 1R4Z[77], 1R50[77], 1T2N[78], 1T4M[78], 1TAH[78], 1YS1[79], 1YS2[79], 2DSN[80], 2ES4[81], 2FX5, 2HIH[82], 2LIP[83], 2NW6[84], 2ORY[85], 2QUA[86], 2QUB[86], 2QXT[87], 2QXU[87], 2W22[88], 2Z5G[80], 2Z8X[89], 2Z8Z[89], 2ZJ6[90], 2ZJ7[90], 2ZVD[91], 3A6Z[91], 3A70[91], 3AUK, 3D2A[92], 3D2B[92], 3D2C[92], 3LIP[83], 3QMM[93], 3QZU[94], 3UMJ[95], 3W9U, 4FDM[96], 4FKB, 4FMP, 4GW3[97], 4GXN[97], 4HS9[97], 4LIP[98], 4OPM, 4X6U[99], 4X71[99], 4X7B[99], 4X85[99], 5AH1[100], 5CE5[100], 5CRI[101], 5CT4[101], 5CT6[101], 5CT9[101], 5CTA[101], 5CUR[101], 5H6B[102], 5LIP[98], 5MAL ² [39], 5XPX, 6A12[103], 6CL4[103], 6FZ1[104], 6FZ7[104], 6FZ8[104], 6FZ9[104], 6FZA[104], 6FZC[104], 6FZD[104]
EC 3.1.1.4	phospholipase A ₂	1FAZ[105], 1KP4[105], 1LWB[106], 1QD5[107], 1QD6[107], 1FW2[108], 1FW3[108], 1ILD[109], 1ILZ[109], 1IM[109], 5DQX
EC 3.1.1.5	lysophospholipase	1IVN ⁵ [110], 1J00 ⁵ [110], 1JRL ⁵ [110], 1U8U ⁵ [111], 1V2G ⁵ [111], 5TIC ⁵ [112], 5TID ⁵ [112], 5TIE ⁵ [112], 5TIF ⁵ [112]
EC 3.1.1.6	acetylesterease	2XLB[113], 2XLC[113], 3FVR, 3FVT, 3FYI, 3FYU, 4NS4
EC 3.1.1.11	pectinesterase	1QJV[114], 2NSP[115], 2NST[115], 2NT6[115], 2NT9[115], 2NTB[115], 2NTP[115], 2NTQ[115], 3UW0[116]
EC 3.1.1.17	gluconolactonase	3DR2[117]
EC 3.1.1.20	tannase	3WA6[118], 3WA7[118]

Table 1. Cont.

EC Number	Enzyme Function	PDB Codes
EC 3.1.1.23	acylglycerol lipase	3RLI[119], 3RM3[119], 4KE6[120], 4KE7[120], 4KE8[120], 4KE9[120], 4KEA[120], 4LHE[121], 5XKS
EC 3.1.1.24	3-oxoadipate enol-lactonase	2XUA [122]
EC 3.1.1.25	1,4-lactonase	3MSR, 3OVG
EC 3.1.1.27	4-pyridoxolactonase	3AJ3, 4KEP, 4KEQ
EC 3.1.1.29	aminoacyl-tRNA hydrolase	2PTH[123], 2Z2I[124], 2Z2J[124], 2Z2K[124], 3KJZ, 3KK0, 3NEA[125], 3OFV, 3P2J, 3TCK[126], 3TCN[126], 3TD2[126], 3TD6[126], 3V2I[127], 3VJR[128], 4DHW, 4DJ, 4ERX, 4FNO[129], 4FOP[130], 4FOT[130], 4FYJ[131], 4HOY[130], 4IKO[130], 4JC4[129], 4JWK[130], 4JX9[130], 4Y7[130], 4LIP[98], 4LWQ, 4OLJ, 4P7B[132], 4QAJ[129], 4QBK[129], 4QD3[129], 4QT4[133], 4V95[134], 4YLY[135], 4Z86[136], 4ZXP[136], 5B6J[136], 5EKT, 5GVZ, 5IKE[136], 5IMB[136], 5IVP, 5Y98[137], 5Y9A[137], 5YLA, 5YLA, 5YN4, 5ZK0, 5ZX8[138], 5ZZV, 6A31, 6IVV, 6IX6, 6IYE, 6J93, 6GU, 6J1, 6JQ, 6JKX, 6JQT
EC 3.1.1.31	6-phosphoglucono-lactonase	1PB7, 1VL1 , 3ICO [139], 3LWD , 3OC6 [139], 4TM7[140], 4TM8[140], 6NAU
EC 3.1.1.32	phospholipase A ₁	1QD5[107], 1QD6[107], 1FW2 [108], 1FW3[108], 1ILD[109], 1ILZ[109], 1IM0[109], 4HYQ [141], 5DQX
EC 3.1.1.41	cephalosporin-C deacetylase	1L7A , 1ODS[142], 1ODT[142], 1VLQ[143], 3FCY , 3M81[143], 3M82[143], 3M83[143], 5FDF [144], 5GMA[145], 5HFN[144], 5JIB[146]
EC 3.1.1.43	alpha-amino-acid esterase	1MPX [147], 1NX9[148], 1RYY[148], 2B4K[148], 2B9V [148]
EC 3.1.1.45	carboxymethylene-butenolidase	1DIN[149], 1GGV[150], 1Z16[151], 1Z18 [151], 1Z19[151], 1ZIC[151], 1ZIX[151], 1ZIY[151], 1ZJ4[151], 1ZJ5[151], 4P92[152], 4P93[152], 4U2B[153], 4U2C[153], 4U2D [153], 4U2E[153], 4U2F[153], 4U2G[153]
EC 3.1.1.57	2-pyrone-4,6-dicarboxylate lactonase	4D8L [154]
EC 3.1.1.61	protein-glutamate methylesterase	1CHD [13], 3SFT[155], 3T8Y [156]
EC 3.1.1.72	acetylxyilan esterase	2CC0[157], 2VPT ⁶ [158], 2WAA[22], 2XLB [113], 2XLC[113], 3FCY , 3W7V [159], 4JHL[159], 4JJ4, 4JJ6, 4JKO[159], 4OAO, 4OAP, 5BN1, 5FDF [144], 5GMA[145], 5HFN[144], 5JIB[146]
EC 3.1.1.73	feruloyl esterase	5YAE[160], 5YAL [160]
EC 3.1.1.74	cutinase	4CG1 [161], 4CG2[161], 4CG3[161], 4EB0, 5ZOA, 5ZNO[162]
EC 3.1.1.75	poly(3-hydroxybutyrate) depolymerase	4BRS[163], 4BTV [163], 4BVJ[163], 4BVK[163], 4BVL[163], 4BYM[163]
EC 3.1.1.81	quorom-quenching N-acyl-homoserine lactonase	2A7M [21], 2BR6[164], 2BTN[164], 3DHA[165], 3DHB[165], 3DHC[165], 4J5F[166], 4J5H[166], 5EH9[167], 5EHT[167]
EC 3.1.1.84	cocaine esterase	1JU3[168], 1JU4[168], 1L7Q[45], 1L7R[45], 3IDA[30], 4P08[169]
EC 3.1.1.85	pimeloyl-[acyl-carrier protein] methyl ester esterase	4ETW [170], 4NMW
EC 3.1.1.95	aclacinomycin methylesterase	1Q0R [171], 1Q0Z[171]
EC 3.1.1.101	poly(ethylene terephthalate) hydrolase	5XFY[172], 5XFZ[172], 5XG0 [172], 5XH2[172], 5XH3[172], 5XJH[173], 5YFE[174], 5YNS[173], 6ANE[175], 6EQD[174], 6EQE[174], 6EQF[174], 6EQG[174], 6EQH[174], 6LWL[176], 6LX[176], 6QGC[177]
EC 3.1.1.102	mono(ethylene terephthalate) hydrolase	6QG9[177], 6QGA[177], 6QGB [177]

* PDB codes with superscript and underline have extra-assigned EC numbers corresponding to any additional activities of the CEHs. ¹ = [EC 3.1.2.12]; ² = [EC 3.1.2.2]; ³ [EC 1.---]; ⁴ = [EC 3.4.21.-]; ⁵ = [EC 3.1.2.2, EC 3.1.2.14, EC 3.4.21.- and EC 3.1.2.-]; and ⁶ = [EC 3.2.1.4]). ** Representative PDB codes are highlighted using **bold** characters.

*** PDB codes in [EC 3.1.1.84] are the same proteins with 3I2K PDB code as a cocaine esterase. However, 3I2F, 3I2G, 3I2H, 3I2I, 3I2J and 3I2K were not assigned to [EC 3.1.1.84].

3. Classification of CEHs Based on Substrates

CEHs can be categorized based on substrates, which can be identified by EC number as shown in Table 1. CEHs using lipids as substrates are phospholipases (only PLA₁ [EC 3.1.1.32] and PLA₂ [EC 3.1.1.4]), carboxylesterases (EC 3.1.1.1), lysophospholipases (EC 3.1.1.5) and triacylglycerol lipases (also called true lipases [EC 3.1.1.3]). However, bacterial lipolytic CEHs are not sensitive to alcohol-group substrates, but to acyl chain length. Carboxylesterase (EC 3.1.1.1) also cleaves carboxylic esters, but the length of the acyl chain is much shorter than the substrates of lipases. Enzyme kinetics and lid structure can also be used to distinguish between lipase and carboxylesterase [178]. In general, lipase contains a lid that covers the active site. However, these approaches are controversial, as some carboxylesterases, such as a lid-containing carboxylesterase, contain a lid similar to those found in lipases [72,179,180].

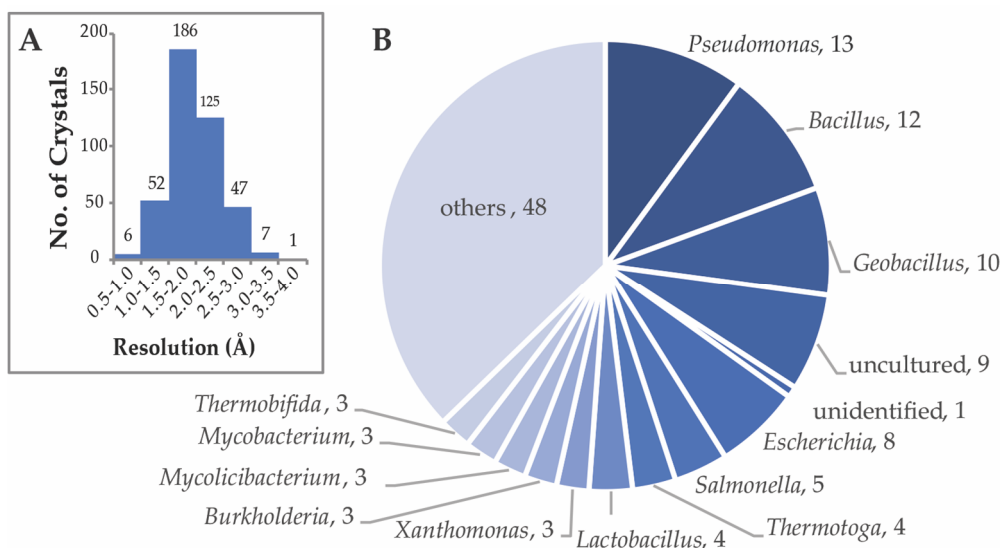


Figure 1. Distribution of the resolution from 424 crystals and the genera of the 136 functionally-annotated CEHs from the PDB are described. (A) The distribution of crystal resolution is shown as a histogram, and the number on top of each bar means the number of crystals in the defined range of resolution. (B) The distribution of genera of CEHs is shown using circle graph. The numbers beside the genera indicate the numbers of CEHs in each genus. When groups have fewer than three members, all are assigned to others.

CEHs that use carbohydrates as substrates are called carbohydrate esterases [181,182]. Carbohydrate esterases that are active on xylan, cutin, and pectin are known as acetylxyran esterase (EC 3.1.1.72), cutinase (EC 3.1.1.74) and pectinesterase (EC 3.1.1.11), respectively, and the acyl chain, most often a member of the acetyl group, is removable in the monomeric and polymeric forms of carbohydrates.

4. Classification Based on Localization

CEHs are distributed from extracellular to cytosolic regions. Ninety of 136 CEHs are localized in the cytosolic region, 43 CEHs have signal peptides for secretion and the remaining three CEHs are transmembrane proteins (Figure 2). Outer membrane phospholipase As (OMPLAs) from *Escherichia coli* (representative PDB code: 1FW2) [107–109] and *Salmonella typhi* (PDB code: 5DQX) span membranes. Autotransporter EstA from *Pseudomonas aeruginosa* (PDB code: 3KVN) is another outer membrane-spanning protein [50]. Representatively, pectin methylesterase from *Dickeya dadantii* (PDB code: 2NSP) with a signal sequence at the N-termini, is a representative secretary CEH for the bacterial invasion of plant tissues [115]. LipA from *Xanthomonas oryzae* (representative PDB code: 3H2G) [28,183], lipase from *Geobacillus zalihae* (PDB code: 2DSN) [80] and phospholipase A₂ from *Streptomyces violaceoruber* (PDB code: 1LWB) [184] have been physiologically verified as secreted proteins, as they can be isolated from culture media.

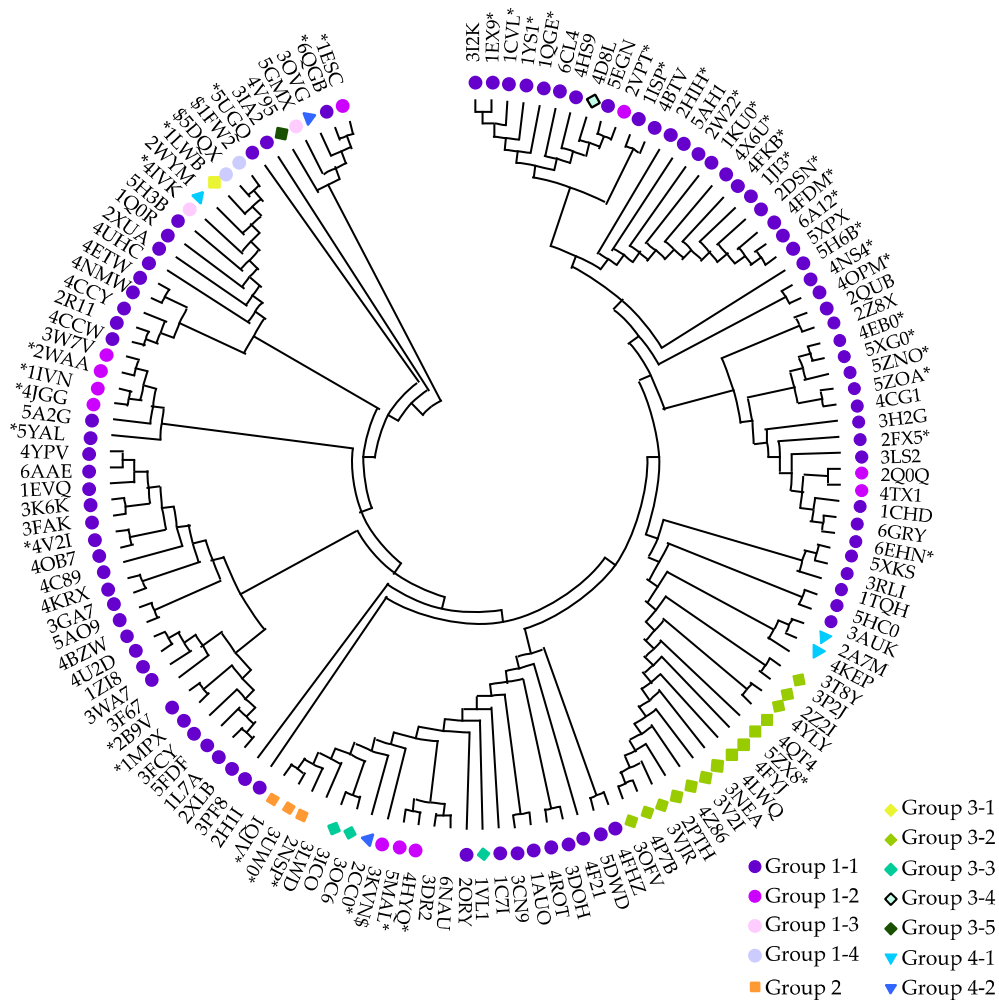


Figure 2. Phylogenetic tree of CEH sequences of all 136 CEHs are aligned and analyzed using a neighbor-joining method and the Jones–Taylor–Thornton (JTT) substitution model. Active site residue-based classification of CEHs is described using a combination of shape and color. Pink-to-purple closed circle: serine hydrolases (Group 1); orangish closed square: aspartidyl hydrolase (Group 2); greenish closed diamond: metal-independent non-serine hydrolases with water molecule as a nucleophile (Group 3); blueish closed triangle: metal-dependent metallohydrolases (Group 4). Different colors are used to distinguish reaction mechanisms. No symbol label means no information is available on their catalytic reaction. Localization of CEHs is described using the following markers at the outside of PDB codes in the phylogenetic tree: Asterisks (*) denote CEHs with signal peptide for secretion and dollar signs (\$) denote membrane protein CEHs. CEHs without a marker are cytosolic CEHs. The figure is prepared using PROMALS3D [185–187] for sequence alignment and MEGA X [188] for phylogenetic tree.

5. Classification Based on the Active Site Residues

Ser-His-Asp in the catalytic triad, which works as a nucleophile, a base and an acid, respectively, is necessary for hydrolysis [189]. In addition to the conventional catalytic triad (Ser-His-Asp), various types of nonconventional triads and dyads have been reported [190]. Gariev et al. classified hydrolases based on components in active sites to produce hierarchical four-digit layers and a web-based database (<http://www.enzyme.chem.msu.ru/hcs>) [191]. In the hydrolysis reaction, O_{γ} in Ser, S_{γ} in Cys, $O_{\gamma 1}$ in Thr, O_{δ} in Asp and O in the water molecule are the nucleophiles, attacking carbonyl carbon in carboxylic ester bonds. The base, usually His residue, deprotonates the nucleophile, and increases the activity of these nucleophiles. The acid stabilizes the position of the base, and assists the function of base to the nucleophile. Along with catalytic residues, the oxyanion hole plays a key role in stabilizing transition

states. CEHs can be classified into several groups based on consensus sequences encompassing their active site residues. Here, we divide CEHs into four groups (groups 1 to 4), based on catalytic residues. Each group is divided into sub-groups according to motifs and conserved residues in the catalytic domain. The information of key residues in each group is provided using the representative structures in Figure 3.

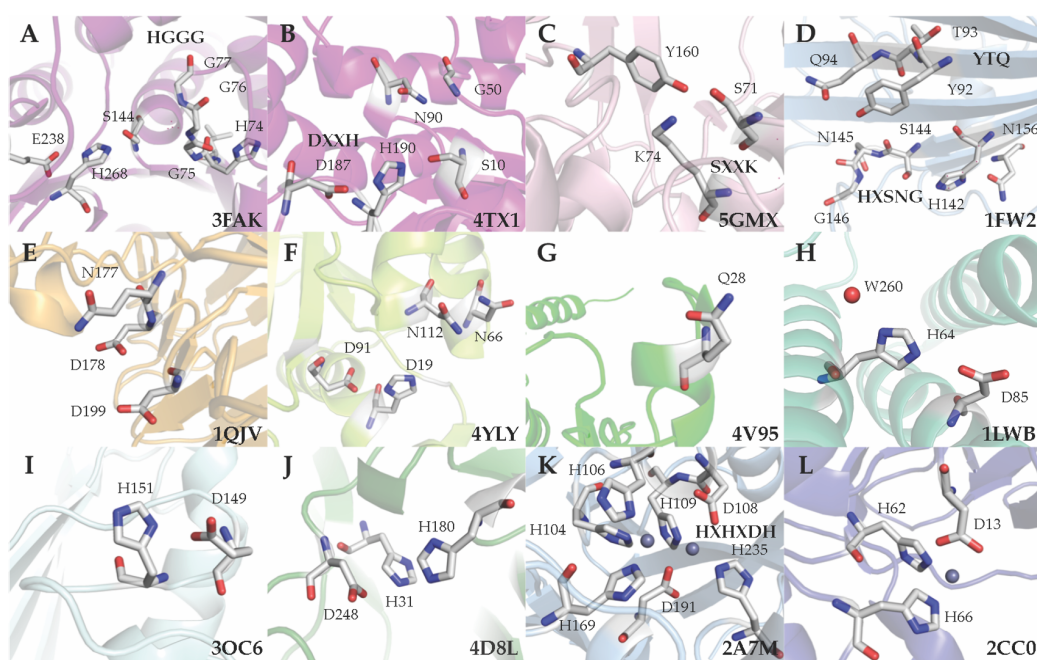


Figure 3. Representative structures of CEHs in groups based on active site are described in 3D structures. The colors in Figure 2 are applied in the cartoon structures of (A) Group 1-1, (B) Group 1-2, (C) Group 1-3, (D) Group 1-4, (E) Group 2, (F) Group 3-1, (G) Group 3-2, (H) Group 3-3, (I) Group 3-4, (J) Group 3-5, (K) Group 4-1 and (L) Group 4-2. Catalytic residues, oxyanion hole residues and important residues are depicted using a sticks model with light gray. The catalytic important water molecule is shown with a red sphere, and metal ions are shown with blue-gray spheres. The names of functional core motifs are depicted near their composing residues. The four-digit PDB codes of the models are noted in bottom-right corner of each panel. Structures are visualized using PyMOL software [192].

5.1. Ser Hydrolases (Group 1)

A sequence analysis of CEHs revealed that many CEHs contain the catalytic triad Ser-His-Asp. We defined group 1 CEHs as those containing the catalytic triad with Ser serving as a nucleophile. Based on motifs containing catalytic Ser, CEHs can be classified into several groups, such as GXSXG, GDSX, SXXK and YTQ/HXSNG groups (underlined residues are nucleophiles). Among them, the GXSXG group is the most common, containing 88 esterases among 136 CEHs.

- Group 1-1

Group 1-1 is the most abundant CEH, and contains the GXSXG motif, along with the AXSXG and GXSXXG variants. The GXSXG motif is localized in the loop region, and forms a catalytic triad with Asp and His in other loops in the C-terminal region. The GXSXXG motif is found in glucuronoyl esterase from *Solibacter usitatus* (PDB code: 6GRY) [42], carbohydrate esterase 15 from a marine metagenome (PDB code: 6EHN) [41], cocaine esterase from *Rhodococcus* spp. (representative PDB code: 3I2K) [29], and alpha-amino acid ester hydrolases from *Acetobacter pasteurianus* (representative PDB code: 2B9V) [148] and *Xanthomonas citri* (PDB code: 1MPX) [147].

Artificial dienelactone hydrolases were obtained through protein engineering, including the mutation of C123S in the GXCXG motif of carboxymethylenebutenolidase from *Pseudomonas knackmussii*

(representative PDB code: 4U2B) [153] and from *Pseudomonas putida* (representative PDB codes: 1ZI8) [151]. Introducing the GXSXG motif reportedly enables the production of an artificial dienelactone hydrolase [193]. The other two triad components are most frequently identified as His-Asp by order in CEHs with GXSXG motifs. Exceptionally, Glu is positioned instead of Asp in the following six CEHs: naproxen esterase from *Bacillus* carboxylesterases cleaving naproxen ester (PDB code: 4CCW) [53], carboxylesterase CesB from *Bacillus sp* (PDB code: 4CCY) [53], Est1 from *Hungatella hathewayi* (PDB code: 5A2G) [37], pNB esterase from *Bacillus subtilis* (PDB code: 1C7I) [19], a putative carboxylesterase from *B. subtilis* (PDB code: 2R11) and metagenomic Est5 (PDB code: 3FAK) [26]. Their catalytic triad therefore is composed of Ser-His-Glu. In this group, the GGGX, GX and Y motifs, which are located mostly in the N-terminal region of a CEH, are involved in forming the oxyanion hole [1,194]. In the GGGX motif, most oxyanion hole components are positioned at the second Gly and third Gly residues. In CEHs containing the GX or Y motifs, with residue X in the GX motif or Tyr in the Y motif, an oxyanion hole forms with the second X in the active site GXSXG motif. In addition, GGAX (representative PDB code: 4V2I [58] and 3DOH [49]) and GAGX (representative PDB code: 1C7I [19], 5A2G [37] and 4C89 [52]) motifs have also been also reported. Y-motif-containing CEHs have been reported in amino acid ester hydrolases (PDB code: 2B9V [148] and 1MPX [147]), and cocaine esterase (representative PDB code: 3I2K [29]). Catalytic His and Asp/Glu are typically positioned with the 20–30 amino acid gap in the order of Asp-His. However, in chemotaxis methylesterase (CheB) from *Salmonella typhimurium* (PDB code: 1CHD), catalytic His190 and D286 are positioned in the reverse order, with 95 unique amino acid gaps [13]. Important residues in this group are shown in Figure 3A.

- Group 1-2

Group 1-2 includes the GDSX motif-containing CEHs (called the GDSL family), in which catalytic Ser is localized close to the N-terminus in a hydrolase domain [196]. According to previous analysis, in the GDSL family, sequence consensus blocks (Block I, II, III and V) contain the functionally important residues Ser, Gly, Asn and His, and thus named SGNH hydrolases, as shown in Figure 4. Catalytic Ser is found in Block I, the oxyanion hole components Gly and Asn are located in Blocks II and III, and a general base known as His exists in Block V (Each residue is marked with an asterisk in Figure 4). The general base His and a general acid Asp form a DXDH motif near the C-terminus of the hydrolase domains. As a rare group, xylan esterase from *Cellvibrio japonicus* (CjCE2A, PDB code: 2WAA) has Asp789 and His791 in a DXH motif (Figure 4) [22].

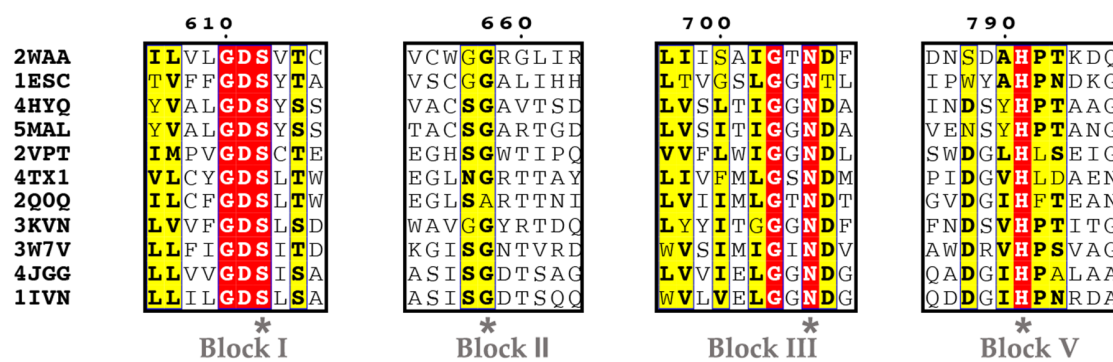


Figure 4. Consensus sequence blocks in the GDSX superfamily. Conserved regions in sequences of the GDSX motif-containing CEHs are described in black-outlined boxes. Assigned numbers above each box are the position of residues in CjCE2A (PDB code: 2WAA) as representative GDSX motif CEHs, and oxyanion hole-forming residues are highlighted using asterisks below the boxes. Fully conserved positions are marked by red shading, and highly conserved positions (>70%) are highlighted in yellow. The conserved residues with high similarity are in bold. PROMALS3D [185–187] for sequence alignment and ESPript 3 [195] for visualization were used.

Moreover, catalytic dyads lacking Asp in the DXXH motif are also identified in lipase from *Streptomyces rimosus* (PDB code: 5MAL) [39] and esterase from *Streptomyces scabies* (PDB code: 1ESC) as shown in Figure 4 [20]. In their structures, Asp residues in the catalytic triad are replaced by nonfunctional Asn in the *S. rimosus* lipase and Trp in the *S. scabies* esterase, in which both Asn and Trp only stabilize the orientation of the catalytic His instead of playing a role as acids. In phospholipase A₁ from *S. albidoflavus* (PDB code: 4HYQ), its sequence shows a conserved DXXH motif of Block V, but the 3D structure reveals that the Ser-His dyads form because of the position of Asp in the DXXH motif is not proper for its function as a general acid [141]. In oxyanion hole formation, aryl esterase from *Mycobacterium smegmatis* (representative PDB code: 2Q0Q) has Ala instead of Gly in Block II, but its function is similar [65]. Important residues in this group are shown in Figure 3B.

- Group 1-3

In group 1-3, the SXXK motif is commonly found in peptidases including β -lactamase [197], and also in family VIII lipases [198,199]. The lipases in family VIII have β -lactamase-like structures, but they usually have carboxylic esterase activity, not β -lactamase activity. Ser71, Lys74 and Tyr160 compose catalytic triads in the EstSRT1, family VIII lipase from the metagenome (PDB code: 5GMX), as in Figure 3C [61]. Another family VIII lipase, EstU1 from the metagenome (PDB code: 4IVK), also has the SXXK motif in which Ser64 and Lys67 form a catalytic triad with Tyr150 [55].

- Group 1-4

Group 1-4 CEHs contain YTQ and HXSNG motifs. OMPLAs from *E. coli* (representative PDB code: 1FW2) [108] and from *S. typhi* (PDB code: 5DQX) belong to this group. The YTQ motif is essential for dimerization of OMPLAs in the membrane, and the HXSNG motif is critical for hydrolase activity [200,201]. In *E. coli* OMPLA, His142 and Ser144 in the HXSNG motif compose a catalytic triad with Asn156, and consecutive Asn145 and Gly146 of the motif are components of an oxyanion hole, as shown in Figure 3D. *S. typhi* OMPLA also has a Ser164-His162-Asn176 catalytic triad and an oxyanion hole formed by Asn165 and Gly166 with the YTQ motif (residues 112–114).

5.2. Aspartyl Hydrolases (Group 2)

Group 2 CEHs are aspartyl hydrolases containing an Asp-Asp dyad with a nucleophilic Asp and a basic Asp, as described in Figure 3E. Epoxide hydrolases [202], and glycosyl hydrolases [203] belong to Asp hydrolases. The Asp-Asp catalytic dyad is also identified in pectin methylesterases (orange squares in Figure 2). Pectin methylesterase A proteins from *Dickeya chrysanthemi* (representative PDB code: 1QJV) [114] and *D. dadanti* (PDB code: 2NSP) [115] contain the GXSXXG motif, although Ser in this motif does not work as a nucleophile. In these enzymes, commonly, Asp199-Asp178 form a catalytic dyad, Gln177 is the oxyanion hole-forming residue, and Arg267 and Trp269 are involved in pectin binding [114,115]. The hydrolysis reaction proceeds metal-independently, and without a nucleophilic water molecule. In a similar manner, in pectin methylesterase (or carbohydrate esterase family VIII) from *Yersinia enterocolitica* (PDB code: 3UW0), Asp199 and Asp177 work as a nucleophile and a general acid/base, respectively [116]. In this enzyme, Arg264 and Trp266 are functionally conserved as a pectin-binding site, and Gln176 belongs to an oxyanion hole [116].

5.3. Metal-independent Hydrolase with a Nucleophilic Water (Group 3)

Group 3 CEHs are nonconventional hydrolases, lacking typical nucleophilic residues such as Ser/Thr/Cys, but containing a water molecule that functions as a nucleophile. The water molecule is activated by general base His (Group 3-1, 3-3 and 3-4), Asp (Group 3-5) and Gln (Group 3-2) residues without metal coordination or the assistance of other cofactors.

- Group 3-1

In the peptidyl-tRNA hydrolase from *Vibrio cholerae* (representative PDB code: 4Z86) belonging to Group 3-1 CEHs, Asn14, His24, Asn72, Asp97 and Asn118 are functionally important [136]. His24 and Asp97 work as a general base and an acid, respectively. Asn72 and Asn118 form an oxyanion hole, and two Asp residues at 14 and 118 stabilize tRNA-binding in its active site. As described in Figure 5, catalytic His-Asp (denoted by an asterisk), two oxyanion hole-forming Asn residues (O-marked) and Asn involved in substrate binding (S-marked) are also conserved in other peptidyl-tRNA hydrolases, such as those from *Mycobacterium tuberculosis* (PDB code: 2Z2I) [124], *M. smegmatis* (PDB code: 3P2J), *E. coli* (PDB code: 3VJR, 2PTH, and 3OFV) [123], *S. typhimurium* (PDB code: 4P7B) [132], *Acinetobacter baumannii* (PDB code: 4LWQ), *Pseudomonas aeruginosa* (PDB code: 4FYJ) [131], *Francisella tularensis* (PDB code: 3NEA) [125], *Streptococcus pyogenes* (PDB code: 4QT4) [133], *Staphylococcus aureus* (PDB code: 4YLY) [135] and *Burkholderia thailandensis* (PDB code: 3V2I) [127]. In the *Thermus thermophilus* peptidyl-tRNA hydrolase (PDB code: 5ZX8), Arg103 plays a role in substrate binding and oxyanion formation similar to Asn118 in *V. cholerae* (Figure 5) [138]. Important residues in this group are shown in Figure 3F.

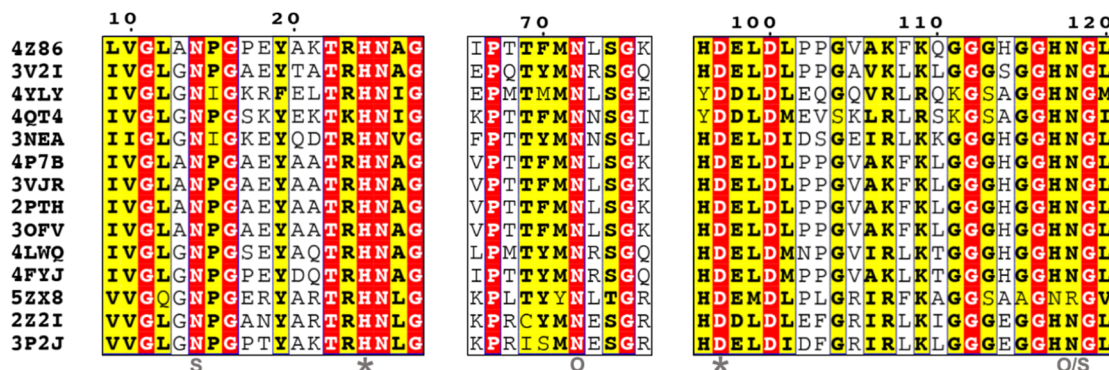


Figure 5. Sequences of peptidyl-tRNA hydrolases are aligned, and functionally important areas are described. The numbers above the sequences are the residual numbers of peptidyl-tRNA hydrolase from *V. cholerae* (PDB 4Z86). Catalytic His and Asp are marked using asterisks, substrate-binding residues are marked using S and oxyanion hole-forming Asn residues are marked using O beneath the sequences. Fully conserved positions are marked with red shading, and highly conserved positions (>70%) are highlighted by yellow shading. The conserved residues with high similarity are in **bold**. PROMALS3D [185–187] for sequence alignment and ESPript 3 [195] for visualization were used.

- Group 3-2

Another type of peptidyl-tRNA hydrolases belonging to the RF-1 family is defined as group 3-2 CEHs in this review (Figure 3G). A common feature of RF-1 family peptidyl-tRNA hydrolase is a GGQ motif. Gln in this motif works as a base that stabilizes nucleophilic water, and also plays a key role in interactions with tRNA [204]. The O_ε1 of Gln28 in YaeJ, a peptidyl-tRNA hydrolase from *E. coli* (PDB code: 4V95) and the nucleophilic water molecule, form a hydrogen bond [134]. The water molecule attacks the carbonyl carbon of the carboxylic ester bond between A76 in tRNA and the peptide.

- Group 3-3

Secreted phospholipase A₂, defined as a group 3-3 CEH, is considered a metal-independent hydrolase using His-Asp as a base-and-acid dyad in the catalytic site to stabilize the nucleophilic water, as shown in Figure 3H [205]. The secreted PLA₂ from *S. violaceoruber* (PDB code: 1LWB) uses His64 and Asp85 as residues in the catalytic dyad and Tyr68 to encourage substrate-binding [106]. In the Ca²⁺-free form of PLA₂ (PDB code: 1LWB), W260 is the inferred nucleophilic water, attacking *sn*-1

carbonyl carbon. In the Ca^{2+} -binding form of PLA₂ (PDB code: 1KP4), the calcium ion, coordinated by O_δ1 of Asp43, O of Leu44, O_δ2 of Asp65 and three water molecules (W201, W202, and W203), induces a hydrogen bond network in a substrate binding pocket. In this enzyme, the water molecule (W256) is regarded as a nucleophile and attacks the *sn*-2 carbonyl carbon of the substrate [105,184].

- Group 3-4

6-phosphogluconolactonases from *M. smegmatis* (representative PDB code: 3OC6) [140] belonging to group 3-4 CEHs contains His151-Glu149 as a catalytic dyad with nucleophilic water (Figure 3I). Similarly, 6-phosphogluconolactonases from *T. tuberculosis* (PDB code: 3ICO) [139] contains His152-Glu150 as a catalytic dyad, and *Thermotoga maritima* 6-phosphogluconolactonase (PDB code: 1VL1) contains the conserved dyad His138-Asp136.

- Group 3-5

Unlike hydrolases described above, the Asp residue of the enzyme belonging to group 3-5 CEH works as a general base on nucleophilic water (Figure 3J). For example, LigI from *Sphingomonas paucimobilis* (PDB code: 4D8L, light green with a black outline in Figure 2) belonging to the amidohydrolase superfamily has lactonase activity using Asp248 as a catalytic base without metal–ion coordination [154]. The water molecule forming a hydrogen bond with Asp248 attacks carbonyl carbon in the lactone group as a nucleophile. His31 and His180 form an oxyanion hole, and His33 contributes to the lactonase reaction by stabilizing the tetrahedral intermediate.

5.4. Metal-dependent Metallohydrolases (Group 4)

- Group 4-1

In the group 4-1 CEH, the HXHXDH motif is involved in Zn^{2+} -binding [206], and His and Asp residues in this motif mainly coordinate the metal ion that stabilizes a nucleophilic water. In *N*-acyl homoserine lactone hydrolase from *Bacillus thuringiensis* (PDB code: 2A7M) [21,166], the HXHXDH motif composed of His104-X-His106-X-Asp108-His109 coordinates two zinc ions with additional Asp191, His169 and His235, as in Figure 3K. The first Zn^{2+} is coordinated by His104, His106 and His169, and the second Zn^{2+} is coordinated by Asp108, His109, Asp191 and His235. According to a known mechanism, one water molecule coordinated by two zinc ions works as a nucleophile, and Tyr194 works as an acid in hydrolysis [24,164]. In 4-pyridoxolactonase from *Mesorhizobium loti* (PDB code: 4KEP), His96, His98, Asp100 and His101 are HXHXDH motif components. Asp100, His101, Asp207 and His252 coordinate the first Zn^{2+} , and His96, His98, His185 and Asp207 coordinate the second Zn^{2+} . In contrast to the HXHXDH-containing group 4-1 CEHs, lactonase UlaG from *E. coli* (representative PDB code: 2WYM) has only one Mn^{2+} at the second Zn^{2+} position, although it has the HXHXDH motif (Figure 6) [23]. HXHXDH motif-containing CEHs are highlighted using the pale blueish-green diamond in Figure 2.

	1 1 0	1 7 0	1 9 0	2 4 0
2A7M	I I S S H L H F D H A	L L Y T P G H S	T I D A S Y	I F F G H D I E Q E
2WYM	V L A T H D H N D H I	L I T T L E A D O	S G D S H Y	V I P F H H D . I W
4KEP	V V N S H F H F D H C	L I S T P G H S	T I D A A Y	L M Y S H D M D N F
	1 1 2 2	1	2	2

Figure 6. The sequences of lactonases containing the HXHXDH motif are aligned. The numbers above the aligned sequences are the residue positions in *N*-acyl lactonase from *Bacillus thuringiensis* (PDB code: 2A7M). The position, which is close to the first and the second metal ions, is marked bottom of the alignment using 1 (the first) and 2 (the second). Fully conserved positions are marked by red shading, and highly conserved positions (>70%) are in yellow. The conserved residues with high similarity are in bold. PROMALS3D [185–187] for sequence alignment and ESPript 3 [195] for visualization are used.

- Group 4-2

This group of CEHs does not contain an HXHXDH motif. For example, the de-O-acetylases family CE4 from *Streptomyces lividans* (PDB code: 2CC0) contains a single Zn²⁺ coordinated by Asp13, His62 and His66 (Figure 3L). For hydrolysis, the nucleophilic water molecule that binds to Zn²⁺ attacks the carbonyl carbon of substrates, and His62 stabilizes the carbonyl group of the substrate by forming an oxyanion hole [157]. Amidohydrolase from *Mycoplasma synoviae* (PDB code: 3OVG) does not have an HXHXDH motif, but two Zn²⁺-binding sites. His186 and His214 coordinate the first Zn²⁺, and His24, His26 and Asp272 coordinate the second Zn²⁺. It also has an His26-Asp68 catalytic dyad.

6. Classification Based on Tertiary Structure

The CATH database (for class, homology, architecture, homologous superfamily; <http://www.cathdb.info>) is designed to predict protein function from structures [207]. In the most recent version of CATH (v4.2.0), a total of 150,885 PDB-deposited structures are classified into four classes, 41 architectures, 1391 topologies and 6119 homologous superfamilies. According to CATH-based analysis, 107 structures of CEHs are classified into an $\alpha/\beta/\alpha$ sandwich architecture (Figure 7A).

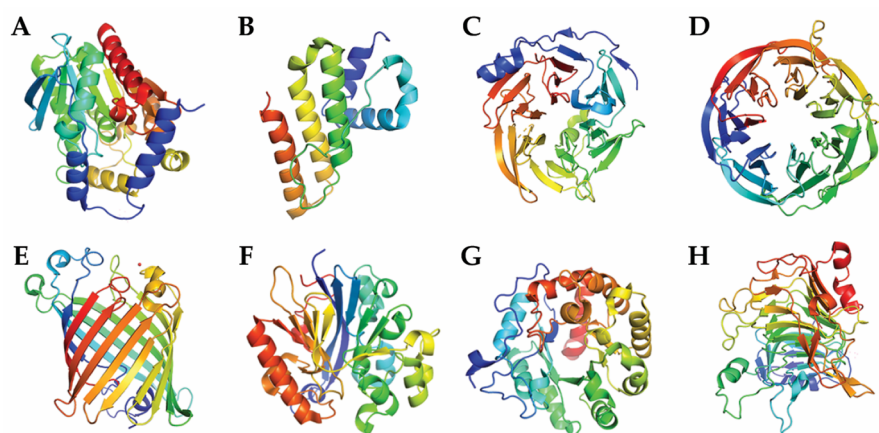


Figure 7. Various tertiary architectures of CEHs in PDB are described using rainbow colors in the direction of the N to C terminus. The 3D models are obtained from representative structures, which contain each architecture: (A) $\alpha/\beta/\alpha$ sandwich (PDB code: 3FAK), (B) up-down bundle (PDB code: 1LWB), (C) 6-blade propeller (PDB code: 3DR2), (D) 7-blade propeller (PDB code: 6NAU), (E) β -barrel (PDB code: 5DQX), (F) $\alpha/\beta/\beta/\alpha$ 4-layer (PDB code: 4KEP), (G) α/β barrel (PDB code: 4D8L), (H) 3-solenoid (PDB code: 2NSP). Structures are visualized using PyMOL software [192].

Among the remaining 29 CEH structures, 16 belong to various architectures, but 13 CEHs (representative PDB codes: 4V95 [134], 5AH1 [100], 5GMX [61], 5H3B [62], 5H6B [102], 5UGQ [40], 5XPX, 5YAL [160], 6A12 [103], 6AAE [63], 6EHN [41], 6GRY [42] and 6QGB [177]) are not classified under the CATH database classification. Secreted PLA₂ from *S. violaceoruber* (PDB code: 1LWB) forms an up-down bundle structure with only helices (Figure 7B). Gluconolactonase from *Xanthomonas campestris* (PDB code: 3DR2) is composed of six blades in a propeller structure (Figure 7C) [117], and similarly, the tertiary structure of 6-phosphogluconolactonase from *Klebsiella pneumoniae* (PDB code: 6NAU) is a 7-blade propeller (Figure 7D). *E. coli* OMPLA (representative PDB code: 1FW2) [108] and *S. typhi* OMPLA (PDB code: 5DQX) form β -barrel structures, and contain a catalytic triad at a dimeric interface in the β -barrel transmembrane area (Figure 7E). Lactone hydrolases (PDB code: 4KEP, 2WYM and 2A7M) have an $\alpha/\beta/\beta/\alpha$ 4-layered fold (Figure 7F). The overall shapes of amidohydrolase LigI from *Sphingobium* (PDB code: 4D8L) [154], acetyl xylan esterases from *S. lividans* (PDB code: 2CC0) [157] and amidohydrolase from *M. synoviae* (PDB code: 3OVG) are α/β barrels (Figure 7G). Apo and substrate-binding forms of pectin methylesterase A from *D. chrysanthemi* (representative PDB

code: 1QJV and 2NSP) [114,115] and *Y. enterocolitica* (PDB code: 3UW0) [116] are right-handed parallel β helices, called 3-solenoids (Figure 7H).

The CEH structures can be also classified according to the CASTLE database (<https://castle.cbe.iastate.edu>) in which bacteria, archaea and eukaryote CEHs are clustered into three clans of α/β hydrolase based on the number and order of β -sheets; eight β -sheets arranged with 1-2-4-3-5-6-7-8 order (Clan A, Figure 8A), five β -sheets arranged with 2-1-3-4-5 order (Clan B, Figure 8B) and seven β -sheets arranged with 1-3-2-4-5-6-7 order (Clan C, Figure 8C) β -sheet sequences. In addition, there are two non- α/β hydrolase clans in the CEHs; a six-bladed β -propeller (Clan D) and three α -helix bundle (Clan E) [208]. Initially, the α/β hydrolase fold was described as α helices surrounding eight central β sheets [209], but it was extended to involve variations including a smaller fold composed of five central β sheets and sandwiched α helices [210]. Among 136 CEHs, 46 structures (33.8%) are turned to have an α/β hydrolase fold in Clans A, B and C (Table 2). Only single structure (PDB code: 3DR2) belongs to Clan D, and no structure is assigned to Clan E.

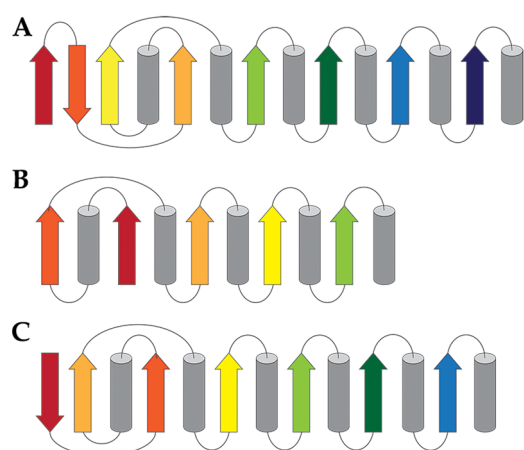


Figure 8. Various topologies of α/β hydrolases in CEHs are described. (A) Classical α/β hydrolase fold with 1-2-4-3-5-6-7-8 order of β sheets. (B) A variant of α/β hydrolase fold with 1-3-2-4-5-6-7 order of β sheets. (C) Minimal α/β hydrolase fold with 2-1-3-4-5 order of β sheets. β sheets are described with rainbow colors (red to navy blue) by the order of β sheets, and all α helices are described with gray. Structures are visualized using PyMOL software [192].

Table 2. Representative PDB Code List of CEH Clans.

Clan Types	PDB Codes
Clan A	1C7I[19], 1EVQ[44], 1L7A, 1Q0R[171], 2R11, 2XLB[113], 2XUA[122], 3FAK[26], 3FCY, 3GA7, 3K6K, 4CCW[53], 4CCY[53], 4CG1[161], 4EB0, 4KRX[35], 4OB7[36]
Clan B	1CVL[69], 1ESC[20], 1EX9[70], 1JI3[74], 1KU0[75], 1QGE, 1YS1[79], 2DSN[80], 2HIH[82], 2W22[88], 3AUUK, 4FDM[96], 4FKB, 4HS9[211], 4HYQ[141], 4X6U[99]
Clan C	1AUO[43], 1TQH[46], 1ZI8 [151], 3CN9[48], 3F67, 3IA2[67], 3RLI[119], 4ETW[170], 4F21[34], 4FHZ[54], 4NMW, 4U2D[153], 4UHC[57]
Clan D	3DR2[117]
Clan E	N/A

7. Substrate-Structure Connection of CEHs

The development of sequencing technology enables the identification of new enzymes from various organisms, including bacteria, and even from the metagenome [212–216]. Functional annotation of those enzymes has been followed by direct or indirect approaches, such as computational sequence/structure analysis and comparison with characterized enzymes [217]. 3D-Fun [218], MOLMAP descriptors [219], ECAssigner [220], EC-blast [221] and the recently released DeepEC [222] have been developed to find links between the EC number and enzyme structures.

Accuracy in predicting the functional assignment of enzymes has improved, but as Gerlt's statistical analysis shows, only 0.63% of proteins by computationally automated annotation have been manually assigned to an EC class [223]. The Ferrer group with the Industrial Applications of Marine Enzymes Consortium (INMARE) attempted to predict enzyme-substrate correlation using the results of a high-throughput assay (145 ester hydrolases sequences and 96 substrates) [224]. Based on this analysis, enzyme promiscuity was proposed. It has been consistently reported that one enzyme can be assigned to multiple classes from primary to quaternary orders of EC class [225]. For example, *E. coli* lysophospholipase L1 (representative PDB code: 1IVN) is assigned to be a lysophospholipase (EC 3.1.1.5), but shows arylesterase (EC 3.1.1.2), palmitoyl-CoA hydrolase (EC 3.1.2.2), acyl-[acyl-carrier-protein] hydrolase (EC 3.1.2.14) and protease (EC 3.4.21.-) activities (Table 1).

8. Physiological Functions of CEHs

Bacterial CEHs participate in various physiological processes, such as signaling pathways, protein synthesis and offensive-defensive responses. Bacteria recognize ligands and respond, moving toward or repelling from ligands through flagellar movement [226]. The response to ligands in surrounding environment conditions occurs using chemotaxis receptors, which are regulated by methyl transferase CheR and hydrolase CheB [14]. CheB removes methyl groups from methylated glutamate residues in the cytoplasm and inactivates receptors. When recognizing high cell density, the Gram-negative bacteria release autoinducers, such as N-acyl homoserine lactone (AHL) derivatives that induce virulence gene expression by self-receptors [227–230]. To remove autoinducing signals, they release AHL lactonase, inactivating and degrading AHL by cleavage lactone rings [16,231]. From the function of lactonase, the regulation of AHL through lactonases has been suggested for medicinal applications [232]. PLAs, including secreted, cytosolic and membrane-integrated forms, work in nutrient digestion, inflammation and intra-signaling cascades [233,234]. Mono- and diacylglycerol lipases are important for lipid metabolism in bacteria [235]. Short-chain fatty acids produced by CEHs in gut microbiota regulate host signaling and metabolic systems [236,237]. In bacterial ribosomal machinery, CEHs also resolve non-stop translation problems by cleaving peptide- or amino acid-conjugated tRNA [238,239].

9. Industrial Applications of CEHs

CEHs are widely used in industrial fields because their endogenous characteristics, such as the substrate specificity and stability of structures [240–243]. Moreover, it has been used for green chemistry, since reactions using biocatalysts employ less steps for the chemical synthesis and produce less harmful wastes during the reaction compared to reactions using chemical catalysts. Furthermore, biocatalysts cover wide substrates with fewer unexpected side products. Carbohydrate esterases have been widely used in animal- and plant-oriented biomass degradation, in the production of biofuels such as ethanol [244–246] and in coffee fermentation to improve flavor and taste [247]. Lipases or carboxylesterases are useful for providing the flavor of yogurt and cheese [248,249]. Polyethylene terephthalate hydrolases are suggested as potent biocatalysts for waste management [250]. These characteristics of CEHs can be further improved through structure-based engineering and directed evolution [251]. Additionally, enzyme reusability through immobilization methods using nanostructure [252], cross-linking [253], encapsulation [254] and entrapment [255], are also being considered, and the immobilized enzymes make it possible to reduce the high initial costs associated with enzyme preparation [256].

10. Perspectives on Identifying More CEHs and Their Functions

CEHs are one of the largest group of enzymes, comprising lipases, carboxylesterases, carbohydrate esterases, peptidyl-tRNA hydrolases and lactonases. They target not only carboxylic ester bonds, but also amide (EC 3.5.1.-), thioester (EC 3.1.2.-) and peroxide (EC 1.---) bonds rarely. The promiscuity of CEHs should be considered when identifying enzyme characteristics.

For these purposes, the factors that induce promiscuity should be identified and the range of specificity chosen. Collecting functional and structural genomics data and linking these large datasets should be done systemically. Amin et al. mentioned the importance of motif in structures when defining enzyme function [257], and Kingsley et al. used various kinetic models to confirm that substrate tunnels in enzymes affect substrate specificity [258]. However, in contrast to an abundance of structural information, fewer structures have been properly matched to biochemical data or functional annotation in the PDB. Moreover, much is unknown about orphan reactions, in which the substrate and the products are already known, but the responsible enzymes are not [259–261]. All existing information should be gathered and used to fill in the remaining blanks to generate a full understanding at the molecular level and draw a heuristic map of the biochemical universe.

Funding: This research was funded by grant from the National Research Foundation of Korea, grant number 2017M3A9E4078553.

Conflicts of Interest: The authors declare no conflict of interest.

References

1. Lian, J.; Nelson, R.; Lehner, R. Carboxylesterases in lipid metabolism: From mouse to human. *Protein Cell* **2018**, *9*, 178–195. [[CrossRef](#)]
2. Soreq, H.; Seidman, S. Acetylcholinesterase—new roles for an old actor. *Nat. Rev. Neurosci.* **2001**, *2*, 294–302. [[CrossRef](#)] [[PubMed](#)]
3. Giudice, E.; Gillet, R. The task force that rescues stalled ribosomes in bacteria. *Trends Biochem. Sci.* **2013**, *38*, 403–411. [[CrossRef](#)] [[PubMed](#)]
4. Pilling, J.; Willmitzer, L.; Fisahn, J. Expression of a *Petunia inflata* pectin methyl esterase in *Solanum tuberosum* l. Enhances stem elongation and modifies cation distribution. *Planta* **2000**, *210*, 391–399. [[CrossRef](#)] [[PubMed](#)]
5. Wu, H.C.; Bulgakov, V.P.; Jinn, T.L. Pectin methylesterases: Cell wall remodeling proteins are required for plant response to heat stress. *Front. Plant Sci.* **2018**, *9*, 1612. [[CrossRef](#)]
6. Schafer, M.; Fischer, C.; Meldau, S.; Seebald, E.; Oelmuller, R.; Baldwin, I.T. Lipase activity in insect oral secretions mediates defense responses in arabidopsis. *Plant Physiol.* **2011**, *156*, 1520–1534. [[CrossRef](#)]
7. Biely, P. Microbial carbohydrate esterases deacetylating plant polysaccharides. *Biotechnol. Adv.* **2012**, *30*, 1575–1588. [[CrossRef](#)]
8. Gendrin, C.; Contreras-Martel, C.; Bouillot, S.; Elsen, S.; Lemaire, D.; Skoufias, D.A.; Huber, P.; Attree, I.; Dessen, A. Structural basis of cytotoxicity mediated by the type III secretion toxin exou from *Pseudomonas aeruginosa*. *PLoS Pathog.* **2012**, *8*, e1002637. [[CrossRef](#)]
9. Sitkiewicz, I.; Stockbauer, K.E.; Musser, J.M. Secreted bacterial phospholipase A2 enzymes: Better living through phospholipolysis. *Trends Microbiol.* **2007**, *15*, 63–69. [[CrossRef](#)]
10. Phillips, R.M.; Six, D.A.; Dennis, E.A.; Ghosh, P. In vivo phospholipase activity of the *Pseudomonas aeruginosa* cytotoxin exou and protection of mammalian cells with phospholipase A2 inhibitors. *J. Biol. Chem.* **2003**, *278*, 41326–41332. [[CrossRef](#)]
11. Armendáriz-Ruiz, M.; Rodríguez-González, J.A.; Camacho-Ruiz, R.M.; Mateos-Díaz, J.C. Carbohydrate esterases: An overview. In *Lipases and Phospholipases: Methods and Protocols*; Sandoval, G., Ed.; Springer: New York, NY, USA, 2018; pp. 39–68.
12. Casas-Godoy, L.; Duquesne, S.; Bordes, F.; Sandoval, G.; Marty, A. Lipases: An overview. In *Lipases and Phospholipases: Methods and Protocols*; Sandoval, G., Ed.; Humana Press: Totowa, NJ, USA, 2012; pp. 3–30.
13. West, A.H.; Martinez-Hackert, E.; Stock, A.M. Crystal structure of the catalytic domain of the chemotaxis receptor methylesterase, CheB. *J. Mol. Biol.* **1995**, *250*, 276–290. [[CrossRef](#)] [[PubMed](#)]
14. Djordjevic, S.; Goudreau, P.N.; Xu, Q.; Stock, A.M.; West, A.H. Structural basis for methylesterase CheB regulation by a phosphorylation-activated domain. *Proc. Natl. Acad. Sci. USA* **1998**, *95*, 1381–1386. [[CrossRef](#)] [[PubMed](#)]
15. Das, G.; Varshney, U. Peptidyl-tRNA hydrolase and its critical role in protein biosynthesis. *Microbiology* **2006**, *152*, 2191–2195. [[CrossRef](#)] [[PubMed](#)]

16. Dong, Y.H.; Xu, J.L.; Li, X.Z.; Zhang, L.H. AiiA, an enzyme that inactivates the acylhomoserine lactone quorum-sensing signal and attenuates the virulence of *Erwinia carotovora*. *Proc. Natl. Acad. Sci. USA* **2000**, *97*, 3526–3531. [[CrossRef](#)]
17. Berman, H.M.; Westbrook, J.; Feng, Z.; Gilliland, G.; Bhat, T.N.; Weissig, H.; Shindyalov, I.N.; Bourne, P.E. The protein data bank. *Nucleic Acids Res.* **2000**, *28*, 235–242. [[CrossRef](#)]
18. Oh, C.; Ryu, B.; Yoo, W.; Nguyen, D.; Kim, T.; Ha, S.-C.; Kim, T.; Kim, K. Identification and crystallographic analysis of a new carbohydrate acylesterase (SmAcE1) from *Sinorhizobium meliloti*. *Crystals* **2018**, *8*, 12. [[CrossRef](#)]
19. Spiller, B.; Gershenson, A.; Arnold, F.H.; Stevens, R.C. A structural view of evolutionary divergence. *Proc. Natl. Acad. Sci. USA* **1999**, *96*, 12305–12310. [[CrossRef](#)]
20. Wei, Y.; Schottel, J.L.; Derewenda, U.; Swenson, L.; Patkar, S.; Derewenda, Z.S. A novel variant of the catalytic triad in the *Streptomyces scabies* esterase. *Nat. Struct. Biol.* **1995**, *2*, 218–223. [[CrossRef](#)]
21. Liu, D.; Lepore, B.W.; Petsko, G.A.; Thomas, P.W.; Stone, E.M.; Fast, W.; Ringe, D. Three-dimensional structure of the quorum-quenching N-acyl homoserine lactone hydrolase from *Bacillus thuringiensis*. *Proc. Natl. Acad. Sci. USA* **2005**, *102*, 11882–11887. [[CrossRef](#)]
22. Montanier, C.; Money, V.A.; Pires, V.M.; Flint, J.E.; Pinheiro, B.A.; Goyal, A.; Prates, J.A.; Izumi, A.; Stalbrand, H.; Morland, C.; et al. The active site of a carbohydrate esterase displays divergent catalytic and noncatalytic binding functions. *PLoS Biol.* **2009**, *7*, e71. [[CrossRef](#)]
23. Garces, F.; Fernandez, F.J.; Montella, C.; Penya-Soler, E.; Prohens, R.; Aguilar, J.; Baldoma, L.; Coll, M.; Badia, J.; Vega, M.C. Molecular architecture of the Mn²⁺-dependent lactonase ulag reveals an RNase-like metallo-beta-lactamase fold and a novel quaternary structure. *J. Mol. Biol.* **2010**, *398*, 715–729. [[CrossRef](#)] [[PubMed](#)]
24. Momb, J.; Wang, C.; Liu, D.; Thomas, P.W.; Petsko, G.A.; Guo, H.; Ringe, D.; Fast, W. Mechanism of the quorum-quenching lactonase (AiiA) from *Bacillus thuringiensis*. 2. Substrate modeling and active site mutations. *Biochemistry* **2008**, *47*, 7715–7725. [[CrossRef](#)] [[PubMed](#)]
25. Nam, K.H.; Kim, M.Y.; Kim, S.J.; Priyadarshi, A.; Kwon, S.T.; Koo, B.S.; Yoon, S.H.; Hwang, K.Y. Structural and functional analysis of a novel hormone-sensitive lipase from a metagenome library. *Proteins* **2009**, *74*, 1036–1040. [[CrossRef](#)] [[PubMed](#)]
26. Nam, K.H.; Kim, M.Y.; Kim, S.J.; Priyadarshi, A.; Lee, W.H.; Hwang, K.Y. Structural and functional analysis of a novel EstE5 belonging to the subfamily of hormone-sensitive lipase. *Biochem. Biophys. Res. Commun.* **2009**, *379*, 553–556. [[CrossRef](#)] [[PubMed](#)]
27. Nam, K.H.; Kim, S.J.; Priyadarshi, A.; Kim, H.S.; Hwang, K.Y. The crystal structure of an HSL-homolog EstE5 complex with PMSF reveals a unique configuration that inhibits the nucleophile Ser144 in catalytic triads. *Biochem. Biophys. Res. Commun.* **2009**, *389*, 247–250. [[CrossRef](#)]
28. Aparna, G.; Chatterjee, A.; Sonti, R.V.; Sankaranarayanan, R. A cell wall-degrading esterase of *Xanthomonas oryzae* requires a unique substrate recognition module for pathogenesis on rice. *Plant Cell* **2009**, *21*, 1860–1873. [[CrossRef](#)]
29. Narasimhan, D.; Nance, M.R.; Gao, D.; Ko, M.C.; Macdonald, J.; Tamburi, P.; Yoon, D.; Landry, D.M.; Woods, J.H.; Zhan, C.G.; et al. Structural analysis of thermostabilizing mutations of cocaine esterase. *Protein Eng. Des. Sel.* **2010**, *23*, 537–547. [[CrossRef](#)]
30. Brim, R.L.; Nance, M.R.; Youngstrom, D.W.; Narasimhan, D.; Zhan, C.G.; Tesmer, J.J.; Sunahara, R.K.; Woods, J.H. A thermally stable form of bacterial cocaine esterase: A potential therapeutic agent for treatment of cocaine abuse. *Mol. Pharmacol.* **2010**, *77*, 593–600. [[CrossRef](#)]
31. Alterio, V.; Aurilia, V.; Romanelli, A.; Parracino, A.; Saviano, M.; D'Auria, S.; De Simone, G. Crystal structure of an S-formylglutathione hydrolase from *Pseudoalteromonas haloplanktis tac125*. *Biopolymers* **2010**, *93*, 669–677.
32. Lai, K.K.; Stogios, P.J.; Vu, C.; Xu, X.; Cui, H.; Molloy, S.; Savchenko, A.; Yakunin, A.; Gonzalez, C.F. An inserted alpha/beta subdomain shapes the catalytic pocket of *Lactobacillus johnsonii* cinnamoyl esterase. *PLoS ONE* **2011**, *6*, e23269. [[CrossRef](#)]
33. Narasimhan, D.; Collins, G.T.; Nance, M.R.; Nichols, J.; Edwald, E.; Chan, J.; Ko, M.C.; Woods, J.H.; Tesmer, J.J.; Sunahara, R.K. Subunit stabilization and polyethylene glycolation of cocaine esterase improves *in vivo* residence time. *Mol. Pharmacol.* **2011**, *80*, 1056–1065. [[CrossRef](#)] [[PubMed](#)]

34. Filippova, E.V.; Weston, L.A.; Kuhn, M.L.; Geissler, B.; Gehring, A.M.; Armoush, N.; Adkins, C.T.; Minasov, G.; Dubrovska, I.; Shuvalova, L.; et al. Large scale structural rearrangement of a serine hydrolase from *Francisella tularensis* facilitates catalysis. *J. Biol. Chem.* **2013**, *288*, 10522–10535. [CrossRef] [PubMed]
35. Schiefner, A.; Gerber, K.; Brosig, A.; Boos, W. Structural and mutational analyses of Aes, an inhibitor of MalT in *Escherichia coli*. *Proteins* **2014**, *82*, 268–277. [CrossRef] [PubMed]
36. Dou, S.; Kong, X.D.; Ma, B.D.; Chen, Q.; Zhang, J.; Zhou, J.; Xu, J.H. Crystal structures of *Pseudomonas putida* esterase reveal the functional role of residues 187 and 287 in substrate binding and chiral recognition. *Biochem. Biophys. Res. Commun.* **2014**, *446*, 1145–1150. [CrossRef]
37. Perz, V.; Hromic, A.; Baumschlager, A.; Steinkellner, G.; Pavkov-Keller, T.; Gruber, K.; Bleymaier, K.; Zitzenbacher, S.; Zankel, A.; Mayrhofer, C.; et al. An esterase from anaerobic *Clostridium hathewayi* can hydrolyze aliphatic-aromatic polyesters. *Environ. Sci. Technol.* **2016**, *50*, 2899–2907. [CrossRef]
38. Huang, J.; Huo, Y.Y.; Ji, R.; Kuang, S.; Ji, C.; Xu, X.W.; Li, J. Structural insights of a hormone sensitive lipase homologue Est22. *Sci. Rep.* **2016**, *6*, 28550. [CrossRef]
39. Leščić Ašler, I.; Štefanić, Z.; Maršavelski, A.; Vianello, R.; Kojić-Prodić, B. Catalytic dyad in the sgnh hydrolase superfamily: In-depth insight into structural parameters tuning the catalytic process of extracellular lipase from *Streptomyces rimosus*. *ACS Chem. Biol.* **2017**, *12*, 1928–1936. [CrossRef]
40. Naffin-Olivos, J.L.; Daab, A.; White, A.; Goldfarb, N.E.; Milne, A.C.; Liu, D.; Baikovitz, J.; Dunn, B.M.; Rengarajan, J.; Petsko, G.A.; et al. Structure determination of *Mycobacterium tuberculosis* serine protease Hip1 (Rv2224c). *Biochemistry* **2017**, *56*, 2304–2314. [CrossRef]
41. De Santi, C.; Gani, O.A.; Helland, R.; Williamson, A. Structural insight into a CE15 esterase from the marine bacterial metagenome. *Sci. Rep.* **2017**, *7*, 17278. [CrossRef]
42. Arnling Baath, J.; Mazurkewich, S.; Knudsen, R.M.; Poulsen, J.N.; Olsson, L.; Lo Leggio, L.; Larsbrink, J. Biochemical and structural features of diverse bacterial glucuronoyl esterases facilitating recalcitrant biomass conversion. *Biotechnol. Biofuels* **2018**, *11*, 213. [CrossRef]
43. Kim, K.K.; Song, H.K.; Shin, D.H.; Hwang, K.Y.; Choe, S.; Yoo, O.J.; Suh, S.W. Crystal structure of carboxylesterase from *Pseudomonas fluorescens*, an alpha/beta hydrolase with broad substrate specificity. *Structure* **1997**, *5*, 1571–1584. [CrossRef]
44. De Simone, G.; Galdiero, S.; Manco, G.; Lang, D.; Rossi, M.; Pedone, C. A snapshot of a transition state analogue of a novel thermophilic esterase belonging to the subfamily of mammalian hormone-sensitive lipase. *J. Mol. Biol.* **2000**, *303*, 761–771. [CrossRef] [PubMed]
45. Turner, J.M.; Larsen, N.A.; Basran, A.; Barbas, C.F., 3rd; Bruce, N.C.; Wilson, I.A.; Lerner, R.A. Biochemical characterization and structural analysis of a highly proficient cocaine esterase. *Biochemistry* **2002**, *41*, 12297–12307. [CrossRef] [PubMed]
46. Liu, P.; Wang, Y.F.; Ewis, H.E.; Abdelal, A.T.; Lu, C.D.; Harrison, R.W.; Weber, I.T. Covalent reaction intermediate revealed in crystal structure of the *Geobacillus stearothermophilus* carboxylesterase Est30. *J. Mol. Biol.* **2004**, *342*, 551–561. [CrossRef]
47. Mandrich, L.; Menchise, V.; Alterio, V.; De Simone, G.; Pedone, C.; Rossi, M.; Manco, G. Functional and structural features of the oxyanion hole in a thermophilic esterase from *Alicyclobacillus acidocaldarius*. *Proteins* **2008**, *71*, 1721–1731. [CrossRef] [PubMed]
48. Pesaresi, A.; Lamba, D. Insights into the fatty acid chain length specificity of the carboxylesterase PA3859 from *Pseudomonas aeruginosa*: A combined structural, biochemical and computational study. *Biochimie* **2010**, *92*, 1787–1792. [CrossRef]
49. Levinson, M.; Sun, L.; Hendriks, S.; Swinkels, P.; Akveld, T.; Bultema, J.B.; Barendregt, A.; van den Heuvel, R.H.; Dijkstra, B.W.; van der Oost, J.; et al. Crystal structure and biochemical properties of a novel thermostable esterase containing an immunoglobulin-like domain. *J. Mol. Biol.* **2009**, *385*, 949–962. [CrossRef]
50. Van den Berg, B. Crystal structure of a full-length autotransporter. *J. Mol. Biol.* **2010**, *396*, 627–633. [CrossRef]
51. Benavente, R.; Esteban-Torres, M.; Acebron, I.; de Las Rivas, B.; Munoz, R.; Alvarez, Y.; Mancheno, J.M. Structure, biochemical characterization and analysis of the pleomorphism of carboxylesterase Cest-2923 from *Lactobacillus plantarum* wcfs1. *FEBS J.* **2013**, *280*, 6658–6671. [CrossRef]
52. Alvarez, Y.; Esteban-Torres, M.; Cortes-Cabrera, A.; Gago, F.; Acebron, I.; Benavente, R.; Mardo, K.; de Las Rivas, B.; Munoz, R.; Mancheno, J.M. Esterase LpEst1 from *Lactobacillus plantarum*: A novel and atypical member of the alphabeta hydrolase superfamily of enzymes. *PLoS ONE* **2014**, *9*, e92257. [CrossRef]

53. Rozeboom, H.J.; Godinho, L.F.; Nardini, M.; Quax, W.J.; Dijkstra, B.W. Crystal structures of two *Bacillus* carboxylesterases with different enantioselectivities. *Biochim. Biophys. Acta* **2014**, *1844*, 567–575. [CrossRef] [PubMed]
54. Ma, J.; Wu, L.; Guo, F.; Gu, J.; Tang, X.; Jiang, L.; Liu, J.; Zhou, J.; Yu, H. Enhanced enantioselectivity of a carboxyl esterase from *Rhodobacter sphaeroides* by directed evolution. *Appl. Microbiol. Biotechnol.* **2013**, *97*, 4897–4906. [CrossRef] [PubMed]
55. Cha, S.S.; An, Y.J.; Jeong, C.S.; Kim, M.K.; Jeon, J.H.; Lee, C.M.; Lee, H.S.; Kang, S.G.; Lee, J.H. Structural basis for the beta-lactamase activity of EstU1, a family VIII carboxylesterase. *Proteins* **2013**, *81*, 2045–2051. [CrossRef] [PubMed]
56. Kovacic, F.; Granzin, J.; Wilhelm, S.; Kojic-Prodic, B.; Batra-Safferling, R.; Jaeger, K.E. Structural and functional characterisation of TesA—A novel lysophospholipase A from *Pseudomonas aeruginosa*. *PLoS ONE* **2013**, *8*, e69125. [CrossRef] [PubMed]
57. Sayer, C.; Isupov, M.N.; Bonch-Osmolovskaya, E.; Littlechild, J.A. Structural studies of a thermophilic esterase from a new planctomycetes species, *Thermogutta terrifontis*. *FEBS J.* **2015**, *282*, 2846–2857. [CrossRef]
58. De Santi, C.; Leiros, H.K.; Di Scala, A.; de Pascale, D.; Altermark, B.; Willassen, N.P. Biochemical characterization and structural analysis of a new cold-active and salt-tolerant esterase from the marine *Bacterium thalassospira* sp. *Extremophiles* **2016**, *20*, 323–336. [CrossRef]
59. Pereira, M.R.; Maester, T.C.; Mercaldi, G.F.; de Macedo Lemos, E.G.; Hyvonen, M.; Balan, A. From a metagenomic source to a high-resolution structure of a novel alkaline esterase. *Appl. Microbiol. Biotechnol.* **2017**, *101*, 4935–4949. [CrossRef]
60. Sayer, C.; Szabo, Z.; Isupov, M.N.; Ingham, C.; Littlechild, J.A. The structure of a novel thermophilic esterase from the Planctomycetes species, *Thermogutta terrifontis* reveals an open active site due to a minimal ‘cap’ domain. *Front Microbiol.* **2015**, *6*, 1294. [CrossRef]
61. Cha, S.S.; An, Y.J. Crystal structure of EstSRT1, a family VIII carboxylesterase displaying hydrolytic activity toward oxyimino cephalosporins. *Biochem. Biophys. Res. Commun.* **2016**, *478*, 818–824. [CrossRef]
62. Shi, J.; Cao, X.; Chen, Y.; Cronan, J.E.; Guo, Z. An atypical alpha/beta-hydrolase fold revealed in the crystal structure of pimeloyl-acyl carrier protein methyl esterase biog from *Haemophilus influenzae*. *Biochemistry* **2016**, *55*, 6705–6717. [CrossRef]
63. Kim, S.H.; Kang, P.A.; Han, K.; Lee, S.W.; Rhee, S. Crystal structure of chloramphenicol-metabolizing enzyme EstDL136 from a metagenome. *PLoS ONE* **2019**, *14*, e0210298. [CrossRef] [PubMed]
64. Cheeseman, J.D.; Tocilj, A.; Park, S.; Schrag, J.D.; Kazlauskas, R.J. Structure of an aryl esterase from *Pseudomonas fluorescens*. *Acta Crystallogr. D Biol. Crystallogr.* **2004**, *60*, 1237–1243. [CrossRef] [PubMed]
65. Mathews, I.; Soltis, M.; Saldajeno, M.; Ganshaw, G.; Sala, R.; Weyler, W.; Cervin, M.A.; Whited, G.; Bott, R. Structure of a novel enzyme that catalyzes acyl transfer to alcohols in aqueous conditions. *Biochemistry* **2007**, *46*, 8969–8979. [CrossRef] [PubMed]
66. Yin, D.L.; Bernhardt, P.; Morley, K.L.; Jiang, Y.; Cheeseman, J.D.; Purpero, V.; Schrag, J.D.; Kazlauskas, R.J. Switching catalysis from hydrolysis to perhydrolysis in *Pseudomonas fluorescens* esterase. *Biochemistry* **2010**, *49*, 1931–1942. [CrossRef]
67. Jiang, Y.; Morley, K.L.; Schrag, J.D.; Kazlauskas, R.J. Different active-site loop orientation in serine hydrolases versus acyltransferases. *Chembiochem* **2011**, *12*, 768–776. [CrossRef]
68. Kim, K.; Ryu, B.H.; Kim, S.S.; An, D.R.; Ngo, T.D.; Pandian, R.; Kim, K.K.; Kim, T.D. Structural and biochemical characterization of a carbohydrate acetylesterase from *Sinorhizobium meliloti* 1021. *FEBS Lett.* **2015**, *589*, 117–122. [CrossRef]
69. Lang, D.; Hofmann, B.; Haalck, L.; Hecht, H.J.; Spener, F.; Schmid, R.D.; Schomburg, D. Crystal structure of a bacterial lipase from *Chromobacterium viscosum* ATCC 6918 refined at 1.6 Å resolution. *J. Mol. Biol.* **1996**, *259*, 704–717. [CrossRef]
70. Nardini, M.; Lang, D.A.; Liebeton, K.; Jaeger, K.E.; Dijkstra, B.W. Crystal structure of *Pseudomonas aeruginosa* lipase in the open conformation. The prototype for family I.1 of bacterial lipases. *J. Biol. Chem.* **2000**, *275*, 31219–31225. [CrossRef]
71. Luic, M.; Tomic, S.; Lescic, I.; Ljubovic, E.; Sepac, D.; Sunjic, V.; Vitale, L.; Saenger, W.; Kojic-Prodic, B. Complex of *Burkholderia cepacia* lipase with transition state analogue of 1-phenoxy-2-acetoxybutane: Biocatalytic, structural and modelling study. *Eur. J. Biochem.* **2001**, *268*, 3964–3973. [CrossRef]

72. Van Pouderoyen, G.; Eggert, T.; Jaeger, K.E.; Dijkstra, B.W. The crystal structure of *Bacillus subtilis* lipase: A minimal alpha/beta hydrolase fold enzyme. *J. Mol. Biol.* **2001**, *309*, 215–226. [CrossRef]
73. Kawasaki, K.; Kondo, H.; Suzuki, M.; Ohgiya, S.; Tsuda, S. Alternate conformations observed in catalytic serine of *Bacillus subtilis* lipase determined at 1.3 Å resolution. *Acta Crystallogr. D Biol. Crystallogr.* **2002**, *58*, 1168–1174. [CrossRef] [PubMed]
74. Tyndall, J.D.; Sinchaikul, S.; Fothergill-Gilmore, L.A.; Taylor, P.; Walkinshaw, M.D. Crystal structure of a thermostable lipase from *Bacillus stearothermophilus* P1. *J. Mol. Biol.* **2002**, *323*, 859–869. [CrossRef]
75. Jeong, S.T.; Kim, H.K.; Kim, S.J.; Chi, S.W.; Pan, J.G.; Oh, T.K.; Ryu, S.E. Novel zinc-binding center and a temperature switch in the *Bacillus stearothermophilus* L1 lipase. *J. Biol. Chem.* **2002**, *277*, 17041–17047. [CrossRef] [PubMed]
76. Kim, K.K.; Song, H.K.; Shin, D.H.; Hwang, K.Y.; Suh, S.W. The crystal structure of a triacylglycerol lipase from *Pseudomonas cepacia* reveals a highly open conformation in the absence of a bound inhibitor. *Structure* **1997**, *5*, 173–185. [CrossRef]
77. Dröge, M.J.; Boersma, Y.L.; van Pouderoyen, G.; Vrenken, T.E.; Rüggeberg, C.J.; Reetz, M.T.; Dijkstra, B.W.; Quax, W.J. Directed evolution of *Bacillus subtilis* lipase a by use of enantiomeric phosphonate inhibitors: Crystal structures and phage display selection. *ChemBioChem* **2006**, *7*, 149–157. [CrossRef]
78. Acharya, P.; Rajakumara, E.; Sankaranarayanan, R.; Rao, N.M. Structural basis of selection and thermostability of laboratory evolved *Bacillus subtilis* lipase. *J. Mol. Biol.* **2004**, *341*, 1271–1281. [CrossRef]
79. Mezzetti, A.; Schrag, J.D.; Cheong, C.S.; Kazlauskas, R.J. Mirror-image packing in enantiomer discrimination: molecular basis for the enantioselectivity of *B. cepacia* lipase toward 2-methyl-3-phenyl-1-propanol. *Chem. Biol.* **2005**, *12*, 427–437. [CrossRef]
80. Matsumura, H.; Yamamoto, T.; Leow, T.C.; Mori, T.; Salleh, A.B.; Basri, M.; Inoue, T.; Kai, Y.; Rahman, R.N. Novel cation-pi interaction revealed by crystal structure of thermoalkalophilic lipase. *Proteins* **2008**, *70*, 592–598. [CrossRef]
81. Pauwels, K.; Lustig, A.; Wyns, L.; Tommassen, J.; Savvides, S.N.; Van Gelder, P. Structure of a membrane-based steric chaperone in complex with its lipase substrate. *Nat. Struct. Mol. Biol.* **2006**, *13*, 374–375. [CrossRef]
82. Tiesinga, J.J.; van Pouderoyen, G.; Nardini, M.; Ransac, S.; Dijkstra, B.W. Structural basis of phospholipase activity of *Staphylococcus hyicus* lipase. *J. Mol. Biol.* **2007**, *371*, 447–456. [CrossRef]
83. Schrag, J.D.; Li, Y.; Cygler, M.; Lang, D.; Burgdorf, T.; Hecht, H.J.; Schmid, R.; Schomburg, D.; Rydel, T.J.; Oliver, J.D.; et al. The open conformation of a *Pseudomonas* lipase. *Structure* **1997**, *5*, 187–202. [CrossRef]
84. Luic, M.; Stefanic, Z.; Ceilinger, I.; Hodoscek, M.; Janezic, D.; Lenac, T.; Asler, I.L.; Sepac, D.; Tomic, S. Combined X-ray diffraction and QM/MM study of the *Burkholderia cepacia* lipase-catalyzed secondary alcohol esterification. *J. Phys. Chem. B* **2008**, *112*, 4876–4883. [CrossRef] [PubMed]
85. Jung, S.K.; Jeong, D.G.; Lee, M.S.; Lee, J.K.; Kim, H.K.; Ryu, S.E.; Park, B.C.; Kim, J.H.; Kim, S.J. Structural basis for the cold adaptation of psychrophilic M37 lipase from *Photobacterium lipolyticum*. *Proteins* **2008**, *71*, 476–484. [CrossRef] [PubMed]
86. Meier, R.; Drepper, T.; Svensson, V.; Jaeger, K.E.; Baumann, U. A calcium-gated lid and a large beta-roll sandwich are revealed by the crystal structure of extracellular lipase from *Serratia marcescens*. *J. Biol. Chem.* **2007**, *282*, 31477–31483. [CrossRef]
87. Rajakumara, E.; Acharya, P.; Ahmad, S.; Sankaranaryanan, R.; Rao, N.M. Structural basis for the remarkable stability of *Bacillus subtilis* lipase (Lip A) at low pH. *Biochim. Biophys. Acta* **2008**, *1784*, 302–311. [CrossRef]
88. Carrasco-Lopez, C.; Godoy, C.; de Las Rivas, B.; Fernandez-Lorente, G.; Palomo, J.M.; Guisan, J.M.; Fernandez-Lafuente, R.; Martinez-Ripoll, M.; Hermoso, J.A. Activation of bacterial thermoalkalophilic lipases is spurred by dramatic structural rearrangements. *J. Biol. Chem.* **2009**, *284*, 4365–4372. [CrossRef]
89. Angkawidjaja, C.; You, D.J.; Matsumura, H.; Kuwahara, K.; Koga, Y.; Takano, K.; Kanaya, S. Crystal structure of a family I.3 lipase from *Pseudomonas* sp. MIS38 in a closed conformation. *FEBS Lett.* **2007**, *581*, 5060–5064. [CrossRef]
90. Kuwahara, K.; Angkawidjaja, C.; Matsumura, H.; Koga, Y.; Takano, K.; Kanaya, S. Importance of the Ca²⁺-binding sites in the N-catalytic domain of a family I.3 lipase for activity and stability. *Protein Eng. Des. Sel.* **2008**, *21*, 737–744. [CrossRef]
91. Angkawidjaja, C.; Matsumura, H.; Koga, Y.; Takano, K.; Kanaya, S. X-ray crystallographic and MD simulation studies on the mechanism of interfacial activation of a family I.3 lipase with two lids. *J. Mol. Biol.* **2010**, *400*, 82–95. [CrossRef]

92. Ahmad, S.; Kamal, M.Z.; Sankaranarayanan, R.; Rao, N.M. Thermostable *Bacillus subtilis* lipases: *In vitro* evolution and structural insight. *J. Mol. Biol.* **2008**, *381*, 324–340. [[CrossRef](#)]
93. Kamal, M.Z.; Ahmad, S.; Molugu, T.R.; Vijayalakshmi, A.; Deshmukh, M.V.; Sankaranarayanan, R.; Rao, N.M. In vitro evolved non-aggregating and thermostable lipase: Structural and thermodynamic investigation. *J. Mol. Biol.* **2011**, *413*, 726–741. [[CrossRef](#)] [[PubMed](#)]
94. Augustyniak, W.; Brzezinska, A.A.; Pijning, T.; Wienk, H.; Boelens, R.; Dijkstra, B.W.; Reetz, M.T. Biophysical characterization of mutants of *Bacillus subtilis* lipase evolved for thermostability: Factors contributing to increased activity retention. *Protein Sci.* **2012**, *21*, 487–497. [[CrossRef](#)] [[PubMed](#)]
95. Ruslan, R.; Abd Rahman, R.N.; Leow, T.C.; Ali, M.S.; Basri, M.; Salleh, A.B. Improvement of thermal stability via outer-loop ion pair interaction of mutated T1 lipase from *Geobacillus zalihae* strain T1. *Int. J. Mol. Sci.* **2012**, *13*, 943–960. [[CrossRef](#)] [[PubMed](#)]
96. Abd Rahman, R.N.; Shariff, F.M.; Basri, M.; Salleh, A.B. 3D structure elucidation of thermostable L2 lipase from thermophilic *Bacillus* sp. L2. *Int. J. Mol. Sci.* **2012**, *13*, 9207–9217. [[CrossRef](#)] [[PubMed](#)]
97. Korman, T.P.; Bowie, J.U. Crystal structure of *Proteus mirabilis* lipase, a novel lipase from the *Proteus*/psychrophilic subfamily of lipase family I.I. *PLoS ONE* **2012**, *7*, e52890. [[CrossRef](#)] [[PubMed](#)]
98. Lang, D.A.; Mannesse, M.L.; de Haas, G.H.; Verheij, H.M.; Dijkstra, B.W. Structural basis of the chiral selectivity of *Pseudomonas cepacia* lipase. *Eur. J. Biochem.* **1998**, *254*, 333–340. [[CrossRef](#)] [[PubMed](#)]
99. Dror, A.; Kanteev, M.; Kagan, I.; Gihaz, S.; Shahar, A.; Fishman, A. Structural insights into methanol-stable variants of lipase T6 from *Geobacillus stearothermophilus*. *Appl. Microbiol. Biotechnol.* **2015**, *99*, 9449–9461. [[CrossRef](#)]
100. Perz, V.; Baumschlager, A.; Bleymaier, K.; Zitzenbacher, S.; Hromic, A.; Steinkellner, G.; Pairitsch, A.; Lyskowski, A.; Gruber, K.; Sinkel, C.; et al. Hydrolysis of synthetic polyesters by *Clostridium botulinum* esterases. *Biotechnol. Bioeng.* **2016**, *113*, 1024–1034. [[CrossRef](#)]
101. Nordwald, E.M.; Plaks, J.G.; Snell, J.R.; Sousa, M.C.; Kaar, J.L. Crystallographic investigation of imidazolium ionic liquid effects on enzyme structure. *Chembiochem* **2015**, *16*, 2456–2459. [[CrossRef](#)]
102. Zhao, Z.; Hou, S.; Lan, D.; Wang, X.; Liu, J.; Khan, F.I.; Wang, Y. Crystal structure of a lipase from *Streptomyces* sp. Strain W007—Implications for thermostability and regiospecificity. *FEBS J.* **2017**, *284*, 3506–3519. [[CrossRef](#)]
103. Moharana, T.R.; Pal, B.; Rao, N.M. X-ray structure and characterization of a thermostable lipase from *Geobacillus thermoleovorans*. *Biochem. Biophys. Res. Commun.* **2019**, *508*, 145–151. [[CrossRef](#)] [[PubMed](#)]
104. Gihaz, S.; Kanteev, M.; Pazy, Y.; Fishman, A. Filling the void: Introducing aromatic interactions into solvent tunnels to enhance lipase stability in methanol. *Appl. Microbiol. Biotechnol.* **2018**, *84*, e02143-18. [[CrossRef](#)] [[PubMed](#)]
105. Matoba, Y.; Katsume, Y.; Sugiyama, M. The crystal structure of prokaryotic phospholipase A2. *J. Biol. Chem.* **2002**, *277*, 20059–20069. [[CrossRef](#)] [[PubMed](#)]
106. Matoba, Y.; Sugiyama, M. Atomic resolution structure of prokaryotic phospholipase A2: Analysis of internal motion and implication for a catalytic mechanism. *Proteins* **2003**, *51*, 453–469. [[CrossRef](#)]
107. Snijder, H.J.; Ubarretxena-Belandia, I.; Blaauw, M.; Kalk, K.H.; Verheij, H.M.; Egmond, M.R.; Dekker, N.; Dijkstra, B.W. Structural evidence for dimerization-regulated activation of an integral membrane phospholipase. *Nature* **1999**, *401*, 717–721. [[CrossRef](#)] [[PubMed](#)]
108. Snijder, H.J.; Kingma, R.L.; Kalk, K.H.; Dekker, N.; Egmond, M.R.; Dijkstra, B.W. Structural investigations of calcium binding and its role in activity and activation of outer membrane phospholipase A from *Escherichia coli*. *J. Mol. Biol.* **2001**, *309*, 477–489. [[CrossRef](#)]
109. Snijder, H.J.; Van Eerde, J.H.; Kingma, R.L.; Kalk, K.H.; Dekker, N.; Egmond, M.R.; Dijkstra, B.W. Structural investigations of the active-site mutant Asn156Ala of outer membrane phospholipase A: Function of the Asn-his interaction in the catalytic triad. *Protein Sci.* **2001**, *10*, 1962–1969. [[CrossRef](#)]
110. Lo, Y.C.; Lin, S.C.; Shaw, J.F.; Liaw, Y.C. Crystal structure of *Escherichia coli* thioesterase I/protease I/lysophospholipase L1: Consensus sequence blocks constitute the catalytic center of SGNH-hydrolases through a conserved hydrogen bond network. *J. Mol. Biol.* **2003**, *330*, 539–551. [[CrossRef](#)]
111. Lo, Y.C.; Lin, S.C.; Shaw, J.F.; Liaw, Y.C. Substrate specificities of *Escherichia coli* thioesterase I/protease I/lysophospholipase L1 are governed by its switch loop movement. *Biochemistry* **2005**, *44*, 1971–1979. [[CrossRef](#)]

112. Grisewood, M.J.; Hernandez Lozada, N.J.; Thoden, J.B.; Gifford, N.P.; Mendez-Perez, D.; Schoenberger, H.A.; Allan, M.F.; Floy, M.E.; Lai, R.Y.; Holden, H.M.; et al. Computational redesign of acyl-ACP thioesterase with improved selectivity toward medium-chain-length fatty acids. *ACS Catal.* **2017**, *7*, 3837–3849. [CrossRef]
113. Montoro-García, S.; Gil-Ortiz, F.; García-Carmona, F.; Polo, L.M.; Rubio, V.; Sánchez-Ferrer, Á. The crystal structure of the cephalosporin deacetylating enzyme acetyl xylan esterase bound to paraoxon explains the low sensitivity of this serine hydrolase to organophosphate inactivation. *Biochem. J.* **2011**, *436*, 321–330. [CrossRef] [PubMed]
114. Jenkins, J.; Mayans, O.; Smith, D.; Worboys, K.; Pickersgill, R.W. Three-dimensional structure of *Erwinia chrysanthemi* pectin methylesterase reveals a novel esterase active site. *J. Mol. Biol.* **2001**, *305*, 951–960. [CrossRef] [PubMed]
115. Fries, M.; Ihrig, J.; Brocklehurst, K.; Shevchik, V.E.; Pickersgill, R.W. Molecular basis of the activity of the phytopathogen pectin methylesterase. *EMBO J.* **2007**, *26*, 3879–3887. [CrossRef] [PubMed]
116. Boraston, A.B.; Abbott, D.W. Structure of a pectin methylesterase from *Yersinia enterocolitica*. *Acta Crystallogr. F Struct Biol. Commun.* **2012**, *68*, 129–133. [CrossRef]
117. Chen, C.N.; Chin, K.H.; Wang, A.H.; Chou, S.H. The first crystal structure of gluconolactonase important in the glucose secondary metabolic pathways. *J. Mol. Biol.* **2008**, *384*, 604–614. [CrossRef]
118. Matoba, Y.; Tanaka, N.; Noda, M.; Higashikawa, F.; Kumagai, T.; Sugiyama, M. Crystallographic and mutational analyses of tannase from *Lactobacillus plantarum*. *Proteins* **2013**, *81*, 2052–2058. [CrossRef]
119. Rengachari, S.; Bezerra, G.A.; Riegler-Berket, L.; Gruber, C.C.; Sturm, C.; Taschler, U.; Boeszoermenyi, A.; Dreveny, I.; Zimmermann, R.; Gruber, K.; et al. The structure of monoacylglycerol lipase from *Bacillus* sp. H257 reveals unexpected conservation of the cap architecture between bacterial and human enzymes. *Biochim. Biophys. Acta* **2012**, *1821*, 1012–1021. [CrossRef]
120. Rengachari, S.; Aschauer, P.; Schittmayer, M.; Mayer, N.; Gruber, K.; Breinbauer, R.; Birner-Gruenberger, R.; Dreveny, I.; Oberer, M. Conformational plasticity and ligand binding of bacterial monoacylglycerol lipase. *J. Biol. Chem.* **2013**, *288*, 31093–31104. [CrossRef]
121. Tsurumura, T.; Tsuge, H. Substrate selectivity of bacterial monoacylglycerol lipase based on crystal structure. *J. Struct. Funct. Genom.* **2014**, *15*, 83–89. [CrossRef]
122. Bains, J.; Kaufman, L.; Farnell, B.; Boulanger, M.J. A product analog bound form of 3-oxoadipate-enol-lactonase (PcaD) reveals a multifunctional role for the divergent cap domain. *J. Mol. Biol.* **2011**, *406*, 649–658. [CrossRef]
123. Schmitt, E.; Mechulam, Y.; Fromant, M.; Plateau, P.; Blanquet, S. Crystal structure at 1.2 Å resolution and active site mapping of *Escherichia coli* peptidyl-tRNA hydrolase. *EMBO J.* **1997**, *16*, 4760–4769. [CrossRef] [PubMed]
124. Selvaraj, M.; Roy, S.; Singh, N.S.; Sangeetha, R.; Varshney, U.; Vijayan, M. Structural plasticity and enzyme action: Crystal structures of *Mycobacterium tuberculosis* peptidyl-tRNA hydrolase. *J. Mol. Biol.* **2007**, *372*, 186–193. [CrossRef] [PubMed]
125. Clarke, T.E.; Romanov, V.; Lam, R.; Gothe, S.A.; Peddi, S.R.; Razumova, E.B.; Lipman, R.S.; Branstrom, A.A.; Chirgadze, N.Y. Structure of *Francisella tularensis* peptidyl-tRNA hydrolase. *Acta Crystallogr. F Struct. Biol. Commun.* **2011**, *67*, 446–449. [CrossRef] [PubMed]
126. Selvaraj, M.; Ahmad, R.; Varshney, U.; Vijayan, M. Structures of new crystal forms of *Mycobacterium tuberculosis* peptidyl-tRNA hydrolase and functionally important plasticity of the molecule. *Acta Crystallogr. F Struct. Biol. Commun.* **2012**, *68*, 124–128. [CrossRef] [PubMed]
127. Baugh, L.; Gallagher, L.A.; Patrapuvich, R.; Clifton, M.C.; Gardberg, A.S.; Edwards, T.E.; Armour, B.; Begley, D.W.; Dieterich, S.H.; Dranow, D.M.; et al. Combining functional and structural genomics to sample the essential *Burkholderia* structome. *PLoS ONE* **2013**, *8*, e53851. [CrossRef]
128. Ito, K.; Murakami, R.; Mochizuki, M.; Qi, H.; Shimizu, Y.; Miura, K.; Ueda, T.; Uchiimi, T. Structural basis for the substrate recognition and catalysis of peptidyl-tRNA hydrolase. *Nucleic Acids Res.* **2012**, *40*, 10521–10531. [CrossRef] [PubMed]
129. Singh, A.; Kumar, A.; Gautam, L.; Sharma, P.; Sinha, M.; Bhushan, A.; Kaur, P.; Sharma, S.; Arora, A.; Singh, T.P. Structural and binding studies of peptidyl-tRNA hydrolase from *Pseudomonas aeruginosa* provide a platform for the structure-based inhibitor design against peptidyl-tRNA hydrolase. *Biochem. J.* **2014**, *463*, 329–337. [CrossRef] [PubMed]

130. Kaushik, S.; Singh, N.; Yamini, S.; Singh, A.; Sinha, M.; Arora, A.; Kaur, P.; Sharma, S.; Singh, T.P. The mode of inhibitor binding to peptidyl-tRNA hydrolase: Binding studies and structure determination of unbound and bound peptidyl-tRNA hydrolase from *Acinetobacter baumannii*. *PLoS ONE* **2013**, *8*, e67547. [CrossRef]
131. Hughes, R.C.; McFeeters, H.; Coates, L.; McFeeters, R.L. Recombinant production, crystallization and X-ray crystallographic structure determination of the peptidyl-tRNA hydrolase of *Pseudomonas aeruginosa*. *Acta Crystallogr. F Struct. Biol. Commun.* **2012**, *68*, 1472–1476. [CrossRef]
132. Vandavasi, V.; Taylor-Creel, K.; McFeeters, R.L.; Coates, L.; McFeeters, H. Recombinant production, crystallization and X-ray crystallographic structure determination of peptidyl-tRNA hydrolase from *Salmonella typhimurium*. *Acta Crystallogr. F Struct. Biol. Commun.* **2014**, *70*, 872–877. [CrossRef]
133. Singh, A.; Gautam, L.; Sinha, M.; Bhushan, A.; Kaur, P.; Sharma, S.; Singh, T.P. Crystal structure of peptidyl-tRNA hydrolase from a gram-positive bacterium, *Streptococcus pyogenes* at 2.19 Å resolution shows the closed structure of the substrate-binding cleft. *FEBS Open Bio.* **2014**, *4*, 915–922. [CrossRef] [PubMed]
134. Gagnon, M.G.; Seetharaman, S.V.; Bulkley, D.; Steitz, T.A. Structural basis for the rescue of stalled ribosomes: Structure of YaeJ bound to the ribosome. *Science* **2012**, *335*, 1370–1372. [CrossRef] [PubMed]
135. Zhang, F.; Song, Y.; Niu, L.; Teng, M.; Li, X. Crystal structure of *Staphylococcus aureus* peptidyl-tRNA hydrolase at a 2.25 Å resolution. *Acta Biochim. Biophys. Sin. (Shanghai)* **2015**, *47*, 1005–1010. [PubMed]
136. Kabra, A.; Shahid, S.; Pal, R.K.; Yadav, R.; Pulavarti, S.V.; Jain, A.; Tripathi, S.; Arora, A. Unraveling the stereochemical and dynamic aspects of the catalytic site of bacterial peptidyl-tRNA hydrolase. *RNA* **2017**, *23*, 202–216. [CrossRef]
137. Kaushik, S.; Iqbal, N.; Singh, N.; Sikarwar, J.S.; Singh, P.K.; Sharma, P.; Kaur, P.; Sharma, S.; Owais, M.; Singh, T.P. Search of multiple hot spots on the surface of peptidyl-tRNA hydrolase: Structural, binding and antibacterial studies. *Biochem. J.* **2018**, *475*, 547–560. [CrossRef] [PubMed]
138. Matsumoto, A.; Uehara, Y.; Shimizu, Y.; Ueda, T.; Uchiumi, T.; Ito, K. High-resolution crystal structure of peptidyl-tRNA hydrolase from *Thermus thermophilus*. *Proteins* **2019**, *87*, 226–235. [CrossRef]
139. Baugh, L.; Phan, I.; Begley, D.W.; Clifton, M.C.; Armour, B.; Dranow, D.M.; Taylor, B.M.; Muruthi, M.M.; Abendroth, J.; Fairman, J.W.; et al. Increasing the structural coverage of tuberculosis drug targets. *Tuberculosis (Edinb)* **2015**, *95*, 142–148. [CrossRef]
140. Fujieda, N.; Schättli, J.; Stuttfeld, E.; Ohkubo, K.; Maier, T.; Fukuzumi, S.; Ward, T.R. Enzyme repurposing of a hydrolase as an emergent peroxidase upon metal binding. *Chem. Sci.* **2015**, *6*, 4060–4065. [CrossRef]
141. Murayama, K.; Kano, K.; Matsumoto, Y.; Sugimori, D. Crystal structure of phospholipase A1 from *Streptomyces albidoflavus* NA297. *J. Struct. Biol.* **2013**, *182*, 192–196. [CrossRef]
142. Vincent, F.; Charnock, S.J.; Verschueren, K.H.; Turkenburg, J.P.; Scott, D.J.; Offen, W.A.; Roberts, S.; Pell, G.; Gilbert, H.J.; Davies, G.J.; et al. Multifunctional xylooligosaccharide/cephalosporin c deacetylase revealed by the hexameric structure of the *Bacillus subtilis* enzyme at 1.9 Å resolution. *J. Mol. Biol.* **2003**, *330*, 593–606. [CrossRef]
143. Levisson, M.; Han, G.W.; Deller, M.C.; Xu, Q.; Biely, P.; Hendriks, S.; Ten Eyck, L.F.; Flensburg, C.; Roversi, P.; Miller, M.D.; et al. Functional and structural characterization of a thermostable acetyl esterase from *Thermotoga maritima*. *Proteins* **2012**, *80*, 1545–1559. [CrossRef] [PubMed]
144. Singh, M.K.; Manoj, N. An extended loop in CE7 carbohydrate esterase family is dispensable for oligomerization but required for activity and thermostability. *J. Struct. Biol.* **2016**, *194*, 434–445. [CrossRef] [PubMed]
145. Singh, M.K.; Manoj, N. Structural role of a conserved active site cis proline in the *Thermotoga maritima* acetyl esterase from the carbohydrate esterase family 7. *Proteins* **2017**, *85*, 694–708. [CrossRef] [PubMed]
146. Singh, M.K.; Manoj, N. Crystal structure of *Thermotoga maritima* acetyl esterase complex with a substrate analog: Insights into the distinctive substrate specificity in the CE7 carbohydrate esterase family. *Biochem. Biophys. Res. Commun.* **2016**, *476*, 63–68. [CrossRef] [PubMed]
147. Barends, T.R.; Polderman-Tijmes, J.J.; Jekel, P.A.; Hensgens, C.M.; de Vries, E.J.; Janssen, D.B.; Dijkstra, B.W. The sequence and crystal structure of the alpha-amino acid ester hydrolase from *Xanthomonas citri* define a new family of beta-lactam antibiotic acylases. *J. Biol. Chem.* **2003**, *278*, 23076–23084. [CrossRef]
148. Barends, T.R.; Polderman-Tijmes, J.J.; Jekel, P.A.; Williams, C.; Wybenga, G.; Janssen, D.B.; Dijkstra, B.W. Acetobacter turbidans alpha-amino acid ester hydrolase: How a single mutation improves an antibiotic-producing enzyme. *J. Biol. Chem.* **2006**, *281*, 5804–5810. [CrossRef]

149. Pathak, D.; Ollis, D. Refined structure of dienelactone hydrolase at 1.8 Å. *J. Mol. Biol.* **1990**, *214*, 497–525. [[CrossRef](#)]
150. Robinson, A.; Edwards, K.J.; Carr, P.D.; Barton, J.D.; Ewart, G.D.; Ollis, D.L. Structure of the C123S mutant of dienelactone hydrolase (DLH) bound with the PMS moiety of the protease inhibitor phenylmethylsulfonyl fluoride (PMSF). *Acta Crystallogr. D Biol. Crystallogr.* **2000**, *56*, 1376–1384. [[CrossRef](#)]
151. Kim, H.K.; Liu, J.W.; Carr, P.D.; Ollis, D.L. Following directed evolution with crystallography: Structural changes observed in changing the substrate specificity of dienelactone hydrolase. *Acta Crystallogr. D Biol. Crystallogr.* **2005**, *61*, 920–931. [[CrossRef](#)]
152. Porter, J.L.; Carr, P.D.; Collyer, C.A.; Ollis, D.L. Crystallization of dienelactone hydrolase in two space groups: Structural changes caused by crystal packing. *Acta Crystallogr. F Struct. Biol. Commun.* **2014**, *70*, 884–889. [[CrossRef](#)] [[PubMed](#)]
153. Porter, J.L.; Boon, P.L.; Murray, T.P.; Huber, T.B.; Collyer, C.A.; Ollis, D.L. Directed evolution of new and improved enzyme functions using an evolutionary intermediate and multidirectional search. *ACS Chem. Biol.* **2015**, *10*, 611–621. [[CrossRef](#)] [[PubMed](#)]
154. Hobbs, M.E.; Malashkevich, V.; Williams, H.J.; Xu, C.; Sauder, J.M.; Burley, S.K.; Almo, S.C.; Raushel, F.M. Structure and catalytic mechanism of LigI: Insight into the amidohydrolase enzymes of cog3618 and lignin degradation. *Biochemistry* **2012**, *51*, 3497–3507. [[CrossRef](#)] [[PubMed](#)]
155. Cho, K.H.; Crane, B.R.; Park, S.Y. An insight into the interaction mode between CheB and chemoreceptor from two crystal structures of CheB methylesterase catalytic domain. *Biochem. Biophys. Res. Commun.* **2011**, *411*, 69–75. [[CrossRef](#)] [[PubMed](#)]
156. Park, S.Y.; Crane, B.R. Structural insight into the low affinity between *Thermotoga maritima* CheA and CheB compared to their *Escherichia coli/Salmonella typhimurium* counterparts. *Int. J. Biol. Macromol.* **2011**, *49*, 794–800. [[CrossRef](#)]
157. Taylor, E.J.; Gloster, T.M.; Turkenburg, J.P.; Vincent, F.; Brzozowski, A.M.; Dupont, C.; Shareck, F.; Centeno, M.S.; Prates, J.A.; Puchart, V.; et al. Structure and activity of two metal ion-dependent acetylxyylan esterases involved in plant cell wall degradation reveals a close similarity to peptidoglycan deacetylases. *J. Biol. Chem.* **2006**, *281*, 10968–10975. [[CrossRef](#)]
158. Correia, M.A.; Prates, J.A.; Bras, J.; Fontes, C.M.; Newman, J.A.; Lewis, R.J.; Gilbert, H.J.; Flint, J.E. Crystal structure of a cellulosomal family 3 carbohydrate esterase from *Clostridium thermocellum* provides insights into the mechanism of substrate recognition. *J. Mol. Biol.* **2008**, *379*, 64–72. [[CrossRef](#)]
159. Lansky, S.; Alalouf, O.; Solomon, H.V.; Alhassid, A.; Govada, L.; Chayen, N.E.; Belrhali, H.; Shoham, Y.; Shoham, G. A unique octameric structure of Axe2, an intracellular acetyl-xylooligosaccharide esterase from *Geobacillus stearothermophilus*. *Acta Crystallogr. D Biol. Crystallogr.* **2014**, *70*, 261–278. [[CrossRef](#)]
160. Uraji, M.; Tamura, H.; Mizohata, E.; Arima, J.; Wan, K.; Ogawa, K.; Inoue, T.; Hatanaka, T. Loop of streptomyces feruloyl esterase plays an important role in the enzyme's catalyzing the release of ferulic acid from biomass. *Appl. Environ. Microbiol.* **2018**, *84*, e02300–e02317. [[CrossRef](#)]
161. Roth, C.; Wei, R.; Oeser, T.; Then, J.; Follner, C.; Zimmermann, W.; Strater, N. Structural and functional studies on a thermostable polyethylene terephthalate degrading hydrolase from *Thermobifida fusca*. *Appl. Microbiol. Biotechnol.* **2014**, *98*, 7815–7823. [[CrossRef](#)]
162. Numoto, N.; Kamiya, N.; Bekker, G.J.; Yamagami, Y.; Inaba, S.; Ishii, K.; Uchiyama, S.; Kawai, F.; Ito, N.; Oda, M. Structural dynamics of the PET-degrading cutinase-like enzyme from *Saccharomonospora viridis* AHK190 in substrate-bound states elucidates the Ca(2+)-driven catalytic cycle. *Biochemistry* **2018**, *57*, 5289–5300. [[CrossRef](#)]
163. Jendrossek, D.; Hermawan, S.; Subedi, B.; Papageorgiou, A.C. Biochemical analysis and structure determination of *Paucimonas lemoignei* poly(3-hydroxybutyrate) (PHB) depolymerase PhaZ7 mureins reveal the PHB binding site and details of substrate-enzyme interactions. *Mol. Microbiol.* **2013**, *90*, 649–664. [[CrossRef](#)] [[PubMed](#)]
164. Kim, M.H.; Choi, W.C.; Kang, H.O.; Lee, J.S.; Kang, B.S.; Kim, K.J.; Derewenda, Z.S.; Oh, T.K.; Lee, C.H.; Lee, J.K. The molecular structure and catalytic mechanism of a quorum-quenching *N*-acyl-*L*-homoserine lactone hydrolase. *Proc. Natl. Acad. Sci. USA* **2005**, *102*, 17606–17611. [[CrossRef](#)] [[PubMed](#)]
165. Liu, D.; Momb, J.; Thomas, P.W.; Moulin, A.; Petsko, G.A.; Fast, W.; Ringe, D. Mechanism of the quorum-quenching lactonase (AiiA) from *Bacillus thuringiensis*. 1. Product-bound structures. *Biochemistry* **2008**, *47*, 7706–7714. [[CrossRef](#)] [[PubMed](#)]

166. Liu, C.F.; Liu, D.; Momb, J.; Thomas, P.W.; Lajoie, A.; Petsko, G.A.; Fast, W.; Ringe, D. A phenylalanine clamp controls substrate specificity in the quorum-quenching metallo-gamma-lactonase from *Bacillus thuringiensis*. *Biochemistry* **2013**, *52*, 1603–1610. [CrossRef] [PubMed]
167. Yang, G.; Hong, N.; Baier, F.; Jackson, C.J.; Tokuriki, N. Conformational tinkering drives evolution of a promiscuous activity through indirect mutational effects. *Biochemistry* **2016**, *55*, 4583–4593. [CrossRef] [PubMed]
168. Larsen, N.A.; Turner, J.M.; Stevens, J.; Rosser, S.J.; Basran, A.; Lerner, R.A.; Bruce, N.C.; Wilson, I.A. Crystal structure of a bacterial cocaine esterase. *Nat. Struct. Biol.* **2002**, *9*, 17–21. [CrossRef]
169. Fang, L.; Chow, K.M.; Hou, S.; Xue, L.; Chen, X.; Rodgers, D.W.; Zheng, F.; Zhan, C.G. Rational design, preparation, and characterization of a therapeutic enzyme mutant with improved stability and function for cocaine detoxification. *ACS Chem. Biol.* **2014**, *9*, 1764–1772. [CrossRef]
170. Agarwal, V.; Lin, S.; Lukk, T.; Nair, S.K.; Cronan, J.E. Structure of the enzyme-acyl carrier protein (ACP) substrate gatekeeper complex required for biotin synthesis. *Proc. Natl. Acad. Sci. USA* **2012**, *109*, 17406–17411. [CrossRef]
171. Jansson, A.; Niemi, J.; Mantsala, P.; Schneider, G. Crystal structure of aclacinomycin methylesterase with bound product analogues: Implications for anthracycline recognition and mechanism. *J. Biol. Chem.* **2003**, *278*, 39006–39013. [CrossRef]
172. Han, X.; Liu, W.; Huang, J.W.; Ma, J.; Zheng, Y.; Ko, T.P.; Xu, L.; Cheng, Y.S.; Chen, C.C.; Guo, R.T. Structural insight into catalytic mechanism of pet hydrolase. *Nat. Commun.* **2017**, *8*, 2106. [CrossRef]
173. Joo, S.; Cho, I.J.; Seo, H.K.; Son, H.F.; Sagong, H.Y.; Shin, T.J.; Choi, S.Y.; Lee, S.Y.; Kim, K.J. Structural insight into molecular mechanism of poly(ethylene terephthalate) degradation. *Nat. Commun.* **2018**, *9*, 382. [CrossRef] [PubMed]
174. Liu, B.; He, L.; Wang, L.; Li, T.; Li, C.; Liu, H.; Luo, Y.; Bao, R. Protein crystallography and site-direct mutagenesis analysis of the poly(ethylene terephthalate) hydrolase petase from *Ideonella sakaiensis*. *Chembiochem* **2018**, *19*, 1471–1475. [CrossRef] [PubMed]
175. Fecker, T.; Galaz-Davison, P.; Engelberger, F.; Narui, Y.; Sotomayor, M.; Parra, L.P.; Ramírez-Sarmiento, C.A. Active site flexibility as a hallmark for efficient PET degradation by *I. sakaiensis* PETase. *Biophys. J.* **2018**, *114*, 1302–1312. [CrossRef] [PubMed]
176. Liu, C.; Shi, C.; Zhu, S.; Wei, R.; Yin, C.C. Structural and functional characterization of polyethylene terephthalate hydrolase from *Ideonella sakaiensis*. *Biochem. Biophys. Res. Commun.* **2019**, *508*, 289–294. [CrossRef] [PubMed]
177. Palm, G.J.; Reisky, L.; Bottcher, D.; Muller, H.; Michels, E.A.P.; Walczak, M.C.; Berndt, L.; Weiss, M.S.; Bornscheuer, U.T.; Weber, G. Structure of the plastic-degrading *Ideonella sakaiensis* mhetase bound to a substrate. *Nat. Commun.* **2019**, *10*, 1717. [CrossRef]
178. Ali, Y.B.; Verger, R.; Abousalham, A. Lipases or esterases: Does it really matter? Toward a new bio-physico-chemical classification. In *Lipases and Phospholipases: Methods and Protocols*; Sandoval, G., Ed.; Humana Press: Totowa, NJ, USA, 2012; Volume 861, pp. 31–51.
179. Jaeger, K.E.; Ransac, S.; Koch, H.B.; Ferrato, F.; Dijkstra, B.W. Topological characterization and modeling of the 3D structure of lipase from *Pseudomonas aeruginosa*. *FEBS Lett.* **1993**, *332*, 143–149. [CrossRef]
180. Lesuisse, E.; Schanck, K.; Colson, C. Purification and preliminary characterization of the extracellular lipase of *Bacillus subtilis* 168, an extremely basic pH-tolerant enzyme. *Eur. J. Biochem.* **1993**, *216*, 155–160. [CrossRef]
181. Cantarel, B.L.; Coutinho, P.M.; Rancurel, C.; Bernard, T.; Lombard, V.; Henrissat, B. The carbohydrate-active enzymes database (CAZy): An expert resource for glycogenomics. *Nucleic Acids Res.* **2009**, *37*, D233–D238. [CrossRef]
182. Lombard, V.; Golaconda Ramulu, H.; Drula, E.; Coutinho, P.M.; Henrissat, B. The carbohydrate-active enzymes database (CAZy) in 2013. *Nucleic Acids Res.* **2014**, *42*, D490–D495. [CrossRef]
183. Ray, S.K.; Rajeshwari, R.; Sonti, R.V. Mutants of *Xanthomonas oryzae* pv. Oryzae deficient in general secretory pathway are virulence deficient and unable to secrete xylanase. *Mol. Plant Microbe Interact.* **2000**, *13*, 394–401. [CrossRef]
184. Sugiyama, M.; Ohtani, K.; Izuhara, M.; Koike, T.; Suzuki, K.; Imamura, S.; Misaki, H. A novel prokaryotic phospholipase A2. Characterization, gene cloning, and solution structure. *J. Biol. Chem.* **2002**, *277*, 20051–20058. [CrossRef] [PubMed]

185. Pei, J.; Grishin, N.V. PROMALS3D: Multiple protein sequence alignment enhanced with evolutionary and three-dimensional structural information. *Methods Mol. Biol.* **2014**, *1079*, 263–271. [PubMed]
186. Pei, J.; Kim, B.H.; Grishin, N.V. PROMALS3D: A tool for multiple protein sequence and structure alignments. *Nucleic Acids Res.* **2008**, *36*, 2295–2300. [CrossRef] [PubMed]
187. Pei, J.; Tang, M.; Grishin, N.V. PROMALS3D web server for accurate multiple protein sequence and structure alignments. *Nucleic Acids Res.* **2008**, *36*, W30–W34. [CrossRef] [PubMed]
188. Kumar, S.; Stecher, G.; Li, M.; Knyaz, C.; Tamura, K. MEGA X: Molecular evolutionary genetics analysis across computing platforms. *Mol. Biol. Evol.* **2018**, *35*, 1547–1549. [CrossRef]
189. Rauwerdink, A.; Kazlauskas, R.J. How the same core catalytic machinery catalyzes 17 different reactions: The serine-histidine-aspartate catalytic triad of α/β -hydrolase fold enzymes. *ACS Catal.* **2015**, *5*, 6153–6176. [CrossRef]
190. Dodson, G.; Wlodawer, A. Catalytic triads and their relatives. *Trends Biochem. Sci.* **1998**, *23*, 347–352. [CrossRef]
191. Gariev, I.A.; Varfolomeev, S.D. Hierarchical classification of hydrolases catalytic sites. *Bioinformatics* **2006**, *22*, 2574–2576. [CrossRef]
192. DeLano, W.L. *The Pymol Molecular Graphics System*; Delano Scientific: San Carlos, CA, USA, 2002.
193. Walker, I.; Easton, C.J.; Ollis, D.L. Site-directed mutagenesis of dienelactone hydrolase produces dienelactone isomerase. *ChemComm* **2000**, 671–672. [CrossRef]
194. Borrelli, G.M.; Trono, D. Recombinant lipases and phospholipases and their use as biocatalysts for industrial applications. *Int. J. Mol. Sci.* **2015**, *16*, 20774–20840. [CrossRef]
195. Robert, X.; Gouet, P. Deciphering key features in protein structures with the new endscript server. *Nucleic Acids Res.* **2014**, *42*, W320–W324. [CrossRef] [PubMed]
196. Akoh, C.C.; Lee, G.C.; Liaw, Y.C.; Huang, T.H.; Shaw, J.F. GDSL family of serine esterases/lipases. *Prog. Lipid Res.* **2004**, *43*, 534–552. [CrossRef] [PubMed]
197. Goffin, C.; Ghysen, J.M. Biochemistry and comparative genomics of SXXK superfamily acyltransferases offer a clue to the mycobacterial paradox: Presence of penicillin-susceptible target proteins versus lack of efficiency of penicillin as therapeutic agent. *Microbiol. Mol. Biol. Rev.* **2002**, *66*, 702–738. [CrossRef] [PubMed]
198. Arpigny, J.L.; Jaeger, K.E. Bacterial lipolytic enzymes: Classification and properties. *Biochem. J.* **1999**, *343 Pt 1*, 177–183. [CrossRef]
199. Hausmann, S.; Jaeger, K.-E. Lipolytic enzymes from bacteria. In *Handbook of Hydrocarbon and Lipid Microbiology*; Timmis, K.N., Ed.; Springer: Berlin/Heidelberg, Germany, 2010; pp. 1099–1126.
200. Wang, X.; Jiang, F.; Zheng, J.; Chen, L.; Dong, J.; Sun, L.; Zhu, Y.; Liu, B.; Yang, J.; Yang, G.; et al. The outer membrane phospholipase A is essential for membrane integrity and type III secretion in *Shigella flexneri*. *Open Biol.* **2016**, *6*, 160073. [CrossRef]
201. Istivan, T.S.; Coloe, P.J. Phospholipase A in gram-negative bacteria and its role in pathogenesis. *Microbiology* **2006**, *152*, 1263–1274. [CrossRef]
202. Van Loo, B.; Kingma, J.; Arand, M.; Wubbolts, M.G.; Janssen, D.B. Diversity and biocatalytic potential of epoxide hydrolases identified by genome analysis. *Appl. Environ. Microbiol.* **2006**, *72*, 2905–2917. [CrossRef]
203. Davies, G.; Henrissat, B. Structures and mechanisms of glycosyl hydrolases. *Structure* **1995**, *3*, 853–859. [CrossRef]
204. Burroughs, A.M.; Aravind, L. The origin and evolution of release factors: Implications for translation termination, ribosome rescue, and quality control pathways. *Int. J. Mol. Sci.* **2019**, *20*, 1981. [CrossRef]
205. Burke, J.E.; Dennis, E.A. Phospholipase A2 structure/function, mechanism, and signaling. *J. Lipid Res.* **2009**, *50*, S237–S242. [CrossRef]
206. Crichton, R.R. Chapter 12—Zinc—lewis acid and gene regulator. In *Biological Inorganic Chemistry*, 2nd ed.; Crichton, R.R., Ed.; Elsevier: Oxford, UK, 2012; pp. 229–246.
207. Dawson, N.L.; Lewis, T.E.; Das, S.; Lees, J.G.; Lee, D.; Ashford, P.; Orengo, C.A.; Sillitoe, I. CATH: An expanded resource to predict protein function through structure and sequence. *Nucleic Acids Res.* **2016**, *45*, D289–D295. [CrossRef] [PubMed]
208. Chen, Y.; Black, D.S.; Reilly, P.J. Carboxylic ester hydrolases: Classification and database derived from their primary, secondary, and tertiary structures. *Protein Sci.* **2016**, *25*, 1942–1953. [CrossRef] [PubMed]
209. Kourist, R.; Jochens, H.; Bartsch, S.; Kuipers, R.; Padhi, S.K.; Gall, M.; Bottcher, D.; Joosten, H.J.; Bornscheuer, U.T. The alpha/beta-hydrolase fold 3DM database (ABHDB) as a tool for protein engineering. *Chembiochem* **2010**, *11*, 1635–1643. [CrossRef] [PubMed]

210. Heikinheimo, P.; Goldman, A.; Jeffries, C.; Ollis, D.L. Of barn owls and bankers: A lush variety of alpha/beta hydrolases. *Structure* **1999**, *7*, R141–R146. [[CrossRef](#)]
211. Korman, T.P.; Sahachartsiri, B.; Charbonneau, D.M.; Huang, G.L.; Beauregard, M.; Bowie, J.U. Dieselzymes: Development of a stable and methanol tolerant lipase for biodiesel production by directed evolution. *Biotechnol. Biofuels* **2013**, *6*, 70. [[CrossRef](#)] [[PubMed](#)]
212. Solomon, K.V.; Haitjema, C.H.; Thompson, D.A.; O’Malley, M.A. Extracting data from the muck: Deriving biological insight from complex microbial communities and non-model organisms with next generation sequencing. *Curr. Opin. Biotechnol.* **2014**, *28*, 103–110. [[CrossRef](#)]
213. Mukherjee, S.; Seshadri, R.; Varghese, N.J.; Elof-Fadrosh, E.A.; Meier-Kolthoff, J.P.; Goker, M.; Coates, R.C.; Hadjithomas, M.; Pavlopoulos, G.A.; Paez-Espino, D.; et al. 1003 reference genomes of bacterial and archaeal isolates expand coverage of the tree of life. *Nat. Biotechnol.* **2017**, *35*, 676–683. [[CrossRef](#)]
214. Lewin, H.A.; Robinson, G.E.; Kress, W.J.; Baker, W.J.; Coddington, J.; Crandall, K.A.; Durbin, R.; Edwards, S.V.; Forest, F.; Gilbert, M.T.P.; et al. Earth biogenome project: Sequencing life for the future of life. *Proc. Natl. Acad. Sci. USA* **2018**, *115*, 4325–4333. [[CrossRef](#)]
215. Mukherjee, S.; Stamatis, D.; Bertsch, J.; Ovchinnikova, G.; Katta, H.Y.; Mojica, A.; Chen, I.A.; Kyrpides, N.C.; Reddy, T. Genomes Online database (GOLD) v.7: Updates and new features. *Nucleic Acids Res.* **2019**, *47*, D649–D659. [[CrossRef](#)]
216. Koutsandreas, T.; Ladoukakis, E.; Pilalis, E.; Zarafeta, D.; Kolisis, F.N.; Skretas, G.; Chatzioannou, A.A. Anastasia: An automated metagenomic analysis pipeline for novel enzyme discovery exploiting next generation sequencing data. *Front. Genet.* **2019**, *10*, 469. [[CrossRef](#)]
217. Prosser, G.A.; Larrouy-Maumus, G.; de Carvalho, L.P. Metabolomic strategies for the identification of new enzyme functions and metabolic pathways. *EMBO Rep.* **2014**, *15*, 657–669. [[CrossRef](#)] [[PubMed](#)]
218. Von Grothuss, M.; Plewczynski, D.; Vriend, G.; Rychlewski, L. 3D-Fun: Predicting enzyme function from structure. *Nucleic Acids Res.* **2008**, *36*, W303–W307. [[CrossRef](#)] [[PubMed](#)]
219. Latino, D.A.; Aires-de-Sousa, J. Assignment of EC numbers to enzymatic reactions with MOLMAP reaction descriptors and random forests. *J. Chem. Inf. Model.* **2009**, *49*, 1839–1846. [[CrossRef](#)] [[PubMed](#)]
220. Hu, Q.N.; Zhu, H.; Li, X.; Zhang, M.; Deng, Z.; Yang, X.; Deng, Z. Assignment of EC numbers to enzymatic reactions with reaction difference fingerprints. *PLoS ONE* **2012**, *7*, e52901. [[CrossRef](#)] [[PubMed](#)]
221. Rahman, S.A.; Cuesta, S.M.; Furnham, N.; Holliday, G.L.; Thornton, J.M. EC-BLAST: A tool to automatically search and compare enzyme reactions. *Nat. Methods* **2014**, *11*, 171–174. [[CrossRef](#)] [[PubMed](#)]
222. Ryu, J.Y.; Kim, H.U.; Lee, S.Y. Deep learning enables high-quality and high-throughput prediction of enzyme commission numbers. *Proc. Natl. Acad. Sci. USA* **2019**, *116*, 13996–14001. [[CrossRef](#)] [[PubMed](#)]
223. Gerlt, J.A. Genomic enzymology: Web tools for leveraging protein family sequence-function space and genome context to discover novel functions. *Biochemistry* **2017**, *56*, 4293–4308. [[CrossRef](#)]
224. Martinez-Martinez, M.; Coscolin, C.; Santiago, G.; Chow, J.; Stogios, P.J.; Bargiela, R.; Gertler, C.; Navarro-Fernandez, J.; Bollinger, A.; Thies, S.; et al. Determinants and prediction of esterase substrate promiscuity patterns. *ACS Chem. Biol.* **2018**, *13*, 225–234. [[CrossRef](#)]
225. Martinez Cuesta, S.; Rahman, S.A.; Furnham, N.; Thornton, J.M. The classification and evolution of enzyme function. *Biophys. J.* **2015**, *109*, 1082–1086. [[CrossRef](#)]
226. Wadhams, G.H.; Armitage, J.P. Making sense of it all: Bacterial chemotaxis. *Nat. Rev. Mol. Cell Biol.* **2004**, *5*, 1024–1037. [[CrossRef](#)]
227. Miller, M.B.; Bassler, B.L. Quorum sensing in bacteria. *Annu. Rev. Microbiol.* **2001**, *55*, 165–199. [[CrossRef](#)] [[PubMed](#)]
228. Rutherford, S.T.; Bassler, B.L. Bacterial quorum sensing: Its role in virulence and possibilities for its control. *Cold Spring Harb. Perspect. Med.* **2012**, *2*, a012427. [[CrossRef](#)] [[PubMed](#)]
229. Wang, L.H.; Weng, L.X.; Dong, Y.H.; Zhang, L.H. Specificity and enzyme kinetics of the quorum-quenching N-acyl homoserine lactone lactonase (AHL-lactonase). *J. Biol. Chem.* **2004**, *279*, 13645–13651. [[CrossRef](#)] [[PubMed](#)]
230. Papenfort, K.; Bassler, B.L. Quorum sensing signal-response systems in gram-negative bacteria. *Nat. Rev. Microbiol.* **2016**, *14*, 576–588. [[CrossRef](#)]
231. Dong, Y.H.; Wang, L.H.; Xu, J.L.; Zhang, H.B.; Zhang, X.F.; Zhang, L.H. Quenching quorum-sensing-dependent bacterial infection by an N-acyl homoserine lactonase. *Nature* **2001**, *411*, 813–817. [[CrossRef](#)]

232. Remy, B.; Mion, S.; Plener, L.; Elias, M.; Chabriere, E.; Daude, D. Interference in bacterial quorum sensing: A biopharmaceutical perspective. *Front. Pharmacol.* **2018**, *9*, 203. [[CrossRef](#)]
233. Chiurchiù, V.; Leuti, A.; Maccarrone, M. Bioactive lipids and chronic inflammation: Managing the fire within. *Front. Immunol.* **2018**, *9*, 38. [[CrossRef](#)]
234. Bonventre, J.V. Phospholipase A2 and signal transduction. *J. Am. Soc. Nephrol.* **1992**, *3*, 128–150.
235. Rameshwaram, N.R.; Singh, P.; Ghosh, S.; Mukhopadhyay, S. Lipid metabolism and intracellular bacterial virulence: Key to next-generation therapeutics. *Future Microbiol.* **2018**, *13*, 1301–1328. [[CrossRef](#)]
236. Tilg, H.; Zmora, N.; Adolph, T.E.; Elinav, E. The intestinal microbiota fuelling metabolic inflammation. *Nat. Rev. Immunol.* **2019**, *1*–15. [[CrossRef](#)]
237. Makki, K.; Deehan, E.C.; Walter, J.; Backhed, F. The impact of dietary fiber on gut microbiota in host health and disease. *Cell Host Microbe* **2018**, *23*, 705–715. [[CrossRef](#)] [[PubMed](#)]
238. Keiler, K.C.; Feaga, H.A. Resolving nonstop translation complexes is a matter of life or death. *J. Bacteriol.* **2014**, *196*, 2123–2130. [[CrossRef](#)] [[PubMed](#)]
239. Keiler, K.C. Mechanisms of ribosome rescue in bacteria. *Nat. Rev. Microbiol.* **2015**, *13*, 285–297. [[CrossRef](#)] [[PubMed](#)]
240. Littlechild, J.A. Enzymes from extreme environments and their industrial applications. *Front. Bioeng. Biotechnol.* **2015**, *3*, 161. [[CrossRef](#)] [[PubMed](#)]
241. Chapman, J.; Ismail, A.E.; Dinu, C.Z. Industrial applications of enzymes: Recent advances, techniques, and outlooks. *Catalysts* **2018**, *8*, 238. [[CrossRef](#)]
242. Sheldon, R.A.; Woodley, J.M. Role of biocatalysis in sustainable chemistry. *Chem. Rev.* **2018**, *118*, 801–838. [[CrossRef](#)]
243. Sheldon, R.A. Biocatalysis and green chemistry. In *Green Biocatalysis*, 1st ed.; Patel, R.N., Ed.; John Wiley & Sons, Inc.: Hoboken, NJ, USA, 2016; pp. 1–15.
244. Sweeney, M.D.; Xu, F. Biomass converting enzymes as industrial biocatalysts for fuels and chemicals: Recent developments. *Catalysts* **2012**, *2*, 244–263. [[CrossRef](#)]
245. Yeoman, C.J.; Han, Y.; Dodd, D.; Schroeder, C.M.; Mackie, R.I.; Cann, I.K.O. Chapter 1—Thermostable enzymes as biocatalysts in the biofuel industry. In *Advances in Applied Microbiology*; Academic Press: San Diego, CA, USA, 2010; Volume 70, pp. 1–55.
246. Mukherjee, J.; Gupta, M.N. Biocatalysis for biomass valorization. *Sustain. Chem. Process.* **2015**, *3*, 7. [[CrossRef](#)]
247. Haile, M.; Kang, W.H. The role of microbes in coffee fermentation and their impact on coffee quality. *J. Food Qual.* **2019**, *2019*, 6. [[CrossRef](#)]
248. Chen, C.; Zhao, S.; Hao, G.; Yu, H.; Tian, H.; Zhao, G. Role of lactic acid bacteria on the yogurt flavour: A review. *Int. J. Food Prop.* **2017**, *20*, S316–S330. [[CrossRef](#)]
249. Holland, R.; Liu, S.Q.; Crow, V.L.; Delabre, M.L.; Lubbers, M.; Bennett, M.; Norris, G. Esterases of lactic acid bacteria and cheese flavour: Milk fat hydrolysis, alcoholysis and esterification. *Int. Dairy J.* **2005**, *15*, 711–718. [[CrossRef](#)]
250. Kawai, F.; Kawabata, T.; Oda, M. Current knowledge on enzymatic PET degradation and its possible application to waste stream management and other fields. *Appl. Microbiol. Biotechnol.* **2019**, *103*, 4253–4268. [[CrossRef](#)]
251. Bornscheuer, U.T.; Huisman, G.W.; Kazlauskas, R.J.; Lutz, S.; Moore, J.C.; Robins, K. Engineering the third wave of biocatalysis. *Nature* **2012**, *485*, 185–194. [[CrossRef](#)] [[PubMed](#)]
252. Verma, M.L.; Naebe, M.; Barrow, C.J.; Puri, M. Enzyme immobilisation on amino-functionalised multi-walled carbon nanotubes: Structural and biocatalytic characterisation. *PLoS ONE* **2013**, *8*, e73642. [[CrossRef](#)] [[PubMed](#)]
253. Cao, L.; van Rantwijk, F.; Sheldon, R.A. Cross-linked enzyme aggregates: A simple and effective method for the immobilization of penicillin acylase. *Org. Lett.* **2000**, *2*, 1361–1364. [[CrossRef](#)] [[PubMed](#)]
254. Su, F.; Li, G.; Fan, Y.; Yan, Y. Enhanced performance of lipase via microencapsulation and its application in biodiesel preparation. *Sci. Rep.* **2016**, *6*, 29670. [[CrossRef](#)]
255. Mingarro, I.; Gonzalez-Navarro, H.; Braco, L. Trapping of different lipase conformers in water-restricted environments. *Biochemistry* **1996**, *35*, 9935–9944. [[CrossRef](#)]
256. Singh, R.K.; Tiwari, M.K.; Singh, R.; Lee, J.K. From protein engineering to immobilization: Promising strategies for the upgrade of industrial enzymes. *Int. J. Mol. Sci.* **2013**, *14*, 1232–1277. [[CrossRef](#)]

257. Amin, S.R.; Erdin, S.; Ward, R.M.; Lua, R.C.; Lichtarge, O. Prediction and experimental validation of enzyme substrate specificity in protein structures. *Proc. Natl. Acad. Sci. USA* **2013**, *110*, E4195–E4202. [[CrossRef](#)]
258. Kingsley, L.J.; Lill, M.A. Substrate tunnels in enzymes: Structure–function relationships and computational methodology. *Proteins* **2015**, *83*, 599–611. [[CrossRef](#)]
259. Chen, L.; Vitkup, D. Distribution of orphan metabolic activities. *Trends Biotechnol.* **2007**, *25*, 343–348. [[CrossRef](#)] [[PubMed](#)]
260. Yamada, T.; Waller, A.S.; Raes, J.; Zelezniak, A.; Perchat, N.; Perret, A.; Salanoubat, M.; Patil, K.R.; Weissenbach, J.; Bork, P. Prediction and identification of sequences coding for orphan enzymes using genomic and metagenomic neighbours. *Mol. Syst. Biol.* **2012**, *8*, 581. [[CrossRef](#)] [[PubMed](#)]
261. Hadadi, N.; MohammadiPeyhani, H.; Miskovic, L.; Seijo, M.; Hatzimanikatis, V. Enzyme annotation for orphan and novel reactions using knowledge of substrate reactive sites. *Proc. Natl. Acad. Sci. USA* **2019**, *116*, 7298–7307. [[CrossRef](#)] [[PubMed](#)]



© 2019 by the authors. Licensee MDPI, Basel, Switzerland. This article is an open access article distributed under the terms and conditions of the Creative Commons Attribution (CC BY) license (<http://creativecommons.org/licenses/by/4.0/>).